AN EXPERIMENTAL INVESTIGATION OF THE EFFECT OF SURFACE CONDITIONS ON NUCLEATE POOL BOILING HEAT TRANSFER TO LIQUID NITROGEN FROM A HORIZONTAL SURFACE

MICHAEL DAMON MAYNARD

AN EXPERIMENTAL INVESTIGATION OF THE EFFECT OF SURFACE CONDITIONS ON NUCLEATE POOL BOILING HEAT TRANSFER TO LIQUID NITROGEN FROM A HORIZONTAL SURFACE

by

Michael Damon Maynard
Lieutenant, United States Navy
B.S., United States Naval Academy, 1959

Submitted in partial fulfillment
for the degree of

MASTER OF SCIENCE IN MECHANICAL ENGINEERING

from the

UNITED STATES NAVAL POSTGRADUATE SCHOOL
May 1966

ABSTRACT

A system was designed to investigate experimentally the mechanism of nucleate pool boiling heat transfer using commercial grade liquid nitrogen as a working fluid. A circular horizontal flat plate five square centimeters in area was utilized as a boiler surface.

The effect of various surface parameters on the characteristic heat flux versus (T_w-T_s) curve at atmospheric conditions was determined. Surfaces used included a highly polished mirror surface, a mirror surface coated with oxide, a mirror surface coated with grease, a roughened surface, and a roughened surface coated with Teflon, all fabricated from commercial electrical tough pitch copper. The final surface used was a Nickel 200 highly polished mirror surface.

The data from the copper surface with a mirror finish was in agreement with the data of previous investigations. The effects of roughness, contaminants, hysteresis, and boiler surface material were discussed. A comparison was made on incipient boiling heat fluxes. The results indicate that the surface conditions play a major role in nucleate pool boiling heat transfer to liquid nitrogen.

TABLE OF CONTENTS

LIST OF TABLES

LIST OF FIGURES

TABLE OF SYMBOLS AND ABBREVIATIONS

A = Area of Heater Surface Exposed to Liquid

C_w = Specific Heat of Wall

C_{sf} = Empirical Constant from Reference [19] for Fluid Surface Combination

d = differential

h = Heat Transfer Coefficient $(Q/A)/\Delta T$

h_{fg} = Latent Heat of Vaporization

H = Immersion Depth of Thermocouple in Fluid.

k_w = Thermal Conductivity of Wall

P_b = Barometric Pressure

P_c = Barometric Pressure Correction

P_o = Standard Pressure = 760 mm Hg

Q/A = Heat Flux per Unit Area in Boiler Wall

R = Gas Constant

T_o = Saturation Temperature at Standard Pressure P_o (normal boiling point)

T_s = Saturation Temperature at Liquid Pressure

T_w = Temperature at the Boiler Wall Surface

$(T_w - T_s) = \Delta T$ = Temperature Difference Between Boiler Surface and Fluid Saturation Temperature at Liquid Pressure

W = Power

X = Distance of Thermocouple from boiler surface

α = Thermal Diffusivity of Boiler Wall = $\frac{k_w}{\rho_w C_w}$

γ = Specific Weight

ρ_w = Density of Wall Material

SECTION I

INTRODUCTION

Background

Recent technological advances in the space program have brought forth great improvements in the ability to obtain and use cryogenic fluids for modern research and industry. Because of its infancy, however, there is still much left unexplored in the realm of cryogenic heat transfer. The uses for the liquified gasses are as varied as their properties. For instance, liquid nitrogen, because of its relative ease in handling and chemical properties, has been used in quick-freeze food preparation, while research laboratories use it as a combination refrigerant-heat sink. The space program has made extensive use of this coolant as an inert pressurizer. Photographic techniques have been refined using liquid nitrogen. Even the medical profession has found uses for liquid nitrogen in blood and tissue preservation, and in cryosurgery.

All of the above uses result in heat being transferred to the liquid nitrogen. As observed in Figure 1, the heat flux (Q/A) and temperature difference (ΔT) determine the mechanism of heat transfer, whether it be by convection, nucleate or film boiling. Because most uses involve the nucleate boiling regime, it is this region that is the general subject of this investigation.

Previous Research

Previous investigations dealing with nucleate boiling using non-cryogenic fluids have attempted to relate effects of surface conditions, among which are included roughness, effects of contaminants, material, and material history. Historically, Corty and Foust [8] were among the earliest to attempt correlation of the effect of surface roughness on

nucleate boiling heat transfer coefficient, using diethyl ether and n-pentane. Generally, their work showed that the polishing of a copper and nickel test surface affected both the position and slope of the boiling curve. In 1962, Berenson [4] furthered the state of the art by comparing nickel, copper and inconel, with n-pentane using more refined techniques. Others such as Westwater, Clark and Strenge [23] were experimenting with boiling water and high speed motion picture studies of active sites from scratches and pits in order to determine the nucleate boiling mechanism. Surface contaminants were the subject of investigations by Averin (oil coating) [1], while Young and Hummel [26], using water, presented data on the effects of Teflon coatings on a roughened surface.

A theoretical investigation was carried out by Bankoff [3], from which he concluded that nucleation from a homogenous liquid was nearly impossible, but he postulated that nucleation proceeds from a pre-existing vapor phase by analyzing fluids in wetted and unwetted cavities. This postulate is verified by Griffith and Wallis [10] in their classic experiment. Bankoff concluded that for wetted cavities, vapor embryos will collapse completely and the cavities will be nullified as nucleation centers. He further states that if the surface is only partially wetted, there will be some steep walled cavities which retain vapor phase. A slight increase in temperature or decrease in pressure would cause the nucleus to grow spontaneously.

Even with all these efforts, the exact mechanism of boiling and the effects of various parameters are far from being understood. A number of investigators have attempted to correlate data. One of the equations which better accounts for surface variables is that of Rohsenow [19]. In his equation, C_{sf} is an empirically determined constant for the fluid surface combinations, indicating that for a theoretical evaluation there

is a need to point out variables with each and every surface combination. For example, amounts of dissolved and/or adsorbed gasses, impurities, contaminants, and the nature of the heating surfaces may vary from one investigation to another, making correlation extremely difficult.

There has been very little reproducible data presented considering the effects of surface conditions on boiling heat transfer using cryogenic fluids. Summaries of data presented by Seader and Miller [21], and, more recently, by Brentari, Giarratano and Smith [7], indicate a very wide spread in data due to surface conditions alone. It is difficult to correlate experimental results with theory and the variables are hard to separate. This has resulted in many investigations which have been undertaken without control of individual variables.

Objective

The objectives of this research were fourfold: first, to design a suitable test device for determining heat rate (Q/A) versus temperature difference (T_w-T_s) for liquid nitrogen and liquid helium, using as much existing equipment as was consistent with the objectives and budget; second, to establish experimental procedures which would yield reproducible nucleate pool boiling data for a given set of boiler surface conditions with liquid nitrogen; third, to make provision for photographic analysis of bubble nucleation using a high speed camera; fourth, to take data on five copper surfaces to include a highly polished mirror finish, a mirror finish coated with oxide, a mirror finish coated with grease, a roughened surface, and a roughened surface coated with Teflon.

In order to design the equipment to accomplish the objective, the following conditions were established:

1. The working fluid was liquid nitrogen because of its availability in high purities at low cost. In addition, the physical properties were

well tabulated and liquid nitrogen exhibited relative ease in handling.

2. The system was open cycle in that nitrogen was allowed to boil away; however, contamination of the boiler and working fluid from condensing oxygen and moisture was to be minimized.

3. The boiler surface was a horizontal flat plate, because it offered the simplest geometry to analyze, and data was available for comparison. Additionally, this design permitted ease in the regulation of test surface finishes and in changing test surfaces.

4. Provision was made for visual observation of the boiling surface during data collection so that future studies could incorporate high speed motion picture analysis.

5. The system was compatible with liquid helium as a working fluid for subsequent investigations.

6. The system was as safe, simple, and flexible as possible.

With these conditions uppermost in mind, the final design resulted in the apparatus shown schematically in Figure 2. A photograph of the actual system is given in Figure 3. Figures 4, 5, and 6 show an exploded view of the boiler-heater assembly, a sectional drawing of the boiler test sections, and an assembled boiler test section. Figures 7 and 8 are a schematic drawing of the vacuum control system and the temperature sensing system. General cryogenic design background was provided by Scott [22] and White [25] .

SECTION 2

DESCRIPTION OF EQUIPMENT

Boiler Test Section

(1) Heater. An electric heater (Figure 4) was fashioned from a 19 inch long inconel-sheathed (.045 inch diameter) Nichrome wire heating element, manufactured by the American Standard Company. Insulation material between the sheath and the wire was magnesium oxide. This heating wire was wound by hand around a 1/16 inch starting mandrel. Final diameter of the button-shaped heater was slightly less than one inch. Resistence of the heater element was 42 ohms.

Previous experimenters studying boiling heat transfer have had a choice between control of heat flux or control of temperature difference in their investigations; similarly, the choice occurred here. While the control of temperature difference allows a wider range of operation over the characteristic boiling curve, with ease in operating in the transition region (Figure 1), the increased complexity of the apparatus for this initial study, plus the fact that only the nucleate region was under study, justified the use of an electric heater to control heat flux. Data of previous investigations [7] indicated that for a variety of surface materials, expected heat fluxes on the order of a maximum of 20 watts/cm^2 were needed in order to attain the maximum nucleate boiling flux. A boiler surface of five cm^2 was selected as being compatible with this flux stipulation, and available space and heaters. In order to maintain one-dimensional transfer, the heater had to have a dimension very close to the maximum diameter of the boiler.

For the expected heat flux, maximum voltage across the heater was calculated to be 65 volts, with a maximum current of 1.55 amps. The watt density was calculated to be 37.8 watts/$inch^2$ per inch of heater, conform-

ing to standard practice. A density of 45 watts/inch^2 per inch of heater was considered as a maximum for this type heater. A sheathed heater was utilized to reduce any electrical noise in the vicinity of the test surface and to provide a surface capable of withstanding the silver solder braze.

(2) Transition Section. The cylindrically shaped transition section of diameter .9935 inches and length .315 inches (Figure 4) was placed between the heater and the nickel boiler or between the heater and disc in the case of the copper boiler. The function of this section was to even out any heat flux discontinuities from the heater, which was brazed to it using silver solder.

(3) Stainless Steel Disc. The Stainless Steel 321 disc shown in Figure 4, had a thickness of .025 inches with a diameter of 1.00 inches. An exact match to the diameter of the transition section and boiler was compromised, as the disc used could be punched out of sheet stock rather than turned down from larger stock. This disc, used only with the copper boiler surface, provided a thermal resistance, insuring that operation of the heater attached to the copper sample was at the same temperature as when it was attached to the Nickel 200 boiler. This disc was placed between the transition section and boiler test surface and soldered in place.

(4) Boiler Plate. The boiler plate (Figure 4) was cylindrical in shape and was made according to the dimensions shown in Figure 5. The length of each cylinder was selected to give a temperature distribution large enough to determine heat flux density with an error of less than ten percent at maximum heat flux. (See Appendix C for sample calculation.)

(5) Boiler Diaphragm and Enclosure. The boiler diaphragm, used to support the boiler on the enclosure, was .020 inches thick and diameter of 1.78 inches. The enclosure was a hollow capped cylinder of 1.78 inches

O.D. and wall thickness of .035 inches. Both items were made from stainless steel and are pictured in Figure 6. The diaphragm was manufactured with a cylindrical lip .035 inches thick and .125 inches long which fit snugly inside the enclosure and was used to secure a leak-tight braze with relative ease.

The two factors determining the thickness of the diaphragm were strength and high resistance to thermal losses. A compromised dimension of .020 inches provided safety and good thermal characteristics. The heater enclosure was designed for low stresses and to allow room for the associated instrumentation and power wires.

Vacuum Systems

For this investigation two vacuum systems were needed. A medium system (10^{-6}mm Hg) was utilized for thermal insulation of the test boiler and inner dewar, while a low vacuum system (10^{-3}mm Hg) was used for environmental control of the boiler fluid. Both are shown schematically in Figure 2.

(1) Thermal Insulation System. A large capacity Welch Duo-Seal 1402-B Two-stage Mechanical Pump served as a roughing pump for the system and fore-pump for the diffusion pump. Rated capacity was 140 liters/minute of free air displacement with an ultimate vacuum of 10^{-4}mm Hg. The pump was vibration-isolated from the pumping unit, using a mounting platform on four small jacks extending to the floor. A Consolidated Vacuum Corporation MCF 300 Fractionating type Diffusion Pump provided the medium vacuum. The rated capacity was 290 liters/second at 0.4 micron with an ultimated vacuum of $2. \times 10^{-7}$mm Hg. Dow-Corning 705 Silicon Oil was used in the diffusion pump because of its resistance to oxidation and very low backstreaming characteristics.

Safety features installed for diffusion pump protection included a thermal cut-out switch, mounted on the cooling coils of the diffusion pump, and a diaphragm vacuum microswitch, located in the fore-pump line. A liquid nitrogen cold trap was placed between the diffusion pump and the test unit to capture condensable vapors and reduce backstreaming. A $1\frac{1}{2}$ inch O.D. x .035 inches wall stainless steel pipe connected the cold trap to the valve manifold. From the valve manifold, the pipe diameter decreased to $\frac{1}{2}$ inch O.D. An Anaconda copper and Mason-Renshaw stainless steel flexible connector were attached to quick-disconnect couplings leading respectively to the dewar and the test unit to provide ease and speed in assembly.

Wherever possible, stainless steel was used to reduce the problem of outgassing within the system. Standard copper tubing elbows were used in conjunction with the stainless pipes. Viton "A" O-rings were used at all flanges because of their low outgassing characteristic. Thermocouples and power leads for the boiler unit penetrated the vacuum system through a Conax MHC Multiple-hole Packing Gland (ceramic followers with a Teflon sealant). This packing gland assembly and the copper elbow fittings were brazed to the stainless pipes using silver solder.

The electrical design for this vacuum system control is shown in Figure 7. The safety features prevent damage from loss of water, vacuum or electrical power. Loss of water pressure, dangerous in that pump oil could reach the flash point, would cause the diffusion pump wall temperature to rise to above 250°F and thereby open the hold-down control coil circuit and shut down the pump. Similarly, a loss of fore-pump vacuum, which would cause oxidation of the diffusion pump oil, would also open the circuit. This feature also prevented energizing the pump without

sufficient vacuum. A loss of electrical power would also open the hold-down control coil. In all cases of automatic shutdown, manual restart would be required.

The thermal insulation vacuum pumping system with control power was assembled as a separate pumping unit for ease in control, access, and flexibility (Figure 3). With minor modifications, the system could be used as a portable system in other studies. A vacuum on the order of 8×10^{-6}mm Hg or better, attained with relative ease, was used for test runs.

(2) Environmental Control. The mechanical pump for this system, a National Research Corporation type 2S, although rated at only 33 liters/minute, proved very satisfactory. The ultimate vacuum of this pump was 3×10^{-3}mm Hg. A liquid nitrogen cold trap was provided between the pump and the dewar. This vacuum system provided control of the environment in the inner dewar. Prior to a run this pump was used to outgas the test surface and dewar. In future studies, it can be used in studying the effect of reduced pressure on nucleate pool boiling.

Dewars

The inner dewar (I.D. = 3.1 inches), shown schematically in Figure 2, held the working fluid which surrounded the boiler assembly, and was provided with an O-ring and flange for vacuum seal in order to control pressure over the fluid. This dewar was connected to the insulation vacuum system by means of a $\frac{1}{2}$ inch Pyrex-Kovar Housekeeper Seal which was, in turn, connected to the quick-disconnect coupling. A dewar with a "permanent" vacuum was not used, as helium penetrates warm pyrex glass at a slow rate, thereby losing the insulating effect.

The outer dewar (I.D. = 4.7 inches), filled with liquid nitrogen and

used as a radiation and intermediate thermal barrier, was manufactured with a sealed permanent vacuum of 10^{-6}mm Hg. The dewars were each fabricated with a double silvered mirror radiation shield and an off-set, aligned, unsilvered, vertical strip 0.8 inches wide, which allowed for visual observation of the boiler surface during boiling.

This double pyrex dewar arrangement provided the needed containers for controlling the environmental conditions affecting the working fluid. At no time was boiling ever observed from the heater assembly due to radiation energy penetrating either through the unsilvered strip or plastic viewport in the dewar flange as long as both dewars were filled.

Instrumentation

(1) Temperature Sensing. ISA type T copper-constantan thermocouples sheathed with Stainless Steel 304 (sheath O.D. = .041 inches, wire diameter = .007 inches), were selected with special limits of error. These high purity sensors were fabricated five feet long with a grounded junction. An x-ray view of this junction is pictured in Figure 9. Careful attention was given to the selection of good detectors. The temperature difference across the copper boiler test section was expected to be a maximum of 8°K. Accuracy of 0.2°K was desired and space was restricted. Even though iron-constantan thermocouples had a larger electromotive force per degree, a greater degree of accuracy could be attained (Dike [9]) with the copper-constantan combination using the calibration methods outlined in Appendix A.

After calibration, four thermocouples were distributed over the length of the test element (Figure 5). Each was coated with Apiezon "N" vacuum grease, then placed in a .042 inch diameter hole which had previously been filled with this grease. Immersion depth was .37 inches. For this immersion depth, a conduction error of less than .04°K was

expected [2]. The grease provided good thermal contact [18] with the boiler and facilitated the element assembly.

The thermocouple leads were fed through the vacuum support tube and the Conax gland, then attached directly to a rotary switch, eliminating associated small errors of extension leads. A liquid nitrogen reference junction was used to minimize error, and the fluid was agitated in order to prevent stratification. A fifth thermocouple was located in the boiling liquid nitrogen to detect changes in bulk temperature during operation.

The rotary switch and thermocouple junctions were located in a zone box (fabricated from $\frac{1}{2}$ inch plywood), which prevented any undesirable Seebeck emfs. The thermocouple output was amplified by a Hewlett Packard Differential Amplifier, Model 8875 A, and fed to a Hewlett Packard automated D.C. Digital Voltmeter, Model 405C. Amplification was necessary in order to obtain three significant figures from the microvolt thermocouple output, as the minimum voltmeter sensitivity was 0.001 volts.

Care was taken to insure that leads were electronically shielded from external noises to prevent any stray current error (following guidelines outlined by Morrison [15]). An internal signal with variable rate control in the voltmeter keyed a Hewlett Packard Digital Recorder, Model 516 B, which printed the visually displayed digital reading on three inch strip paper (data sheet). A schematic diagram is shown in Figure 7. For calibration of the amplifier-digital voltmeter combination see Appendix A.

(2) Pressure Sensing. Pressure in the vacuum system was monitored at low vacuums with National Research Corporation, Model 724, matched thermocouple gauges and at high vacuums with a NRC, type 724 Cold Cathode Ionization Gauge Control with sensing head 524. While taking data on a particular surface, only the cold cathode gauge was monitored.

SECTION 3

EXPERIMENTAL PROCEDURES

Preparation of Test Surfaces

Because of the complex dependence on surface properties, surface preparation, past history of the boiler, etc., the number of active sites of a given size cannot be predicted either theoretically or experimentally. It is hoped, however, that by describing the surface preparation, the microstructure is sufficiently well defined for use in future duplication or correlation.

A machined boiler test surface (see Figure 4) was brazed to a stainless steel diaphragm while, at the same time, a heater was brazed to the copper distribution plug, both with silver solder (m. p. 1170°F) and ruby flux. Upon cooling, the two partial assemblies were bonded together with Eutecrod 157 solder (m. p. 425°F) (95% tin, 5% silver) with the stainless steel disc used between the copper boiler surface and the distribution plug. The purpose of the lower temperature bond was to allow for separation of the heater for use with another test boiler surface. The surface of this entire assembly was then cleaned to remove flux, checked for continuity in the heater, and polished. A complete assembly is shown in test position in Figure 6.

(1) Mirror Finish. The boiler surface, protruding 0.015 inches above the stainless steel diaphragm, was sanded by pressing against a rotating dry 320 grit carborundum belt. The sample was then rotated 90° stroked by hand in one direction only over 0 emery paper, rotated again 90°, and stroked over 3/0 emery paper, both emerys being dry. Only as many strokes were used as were necessary to remove the marks from the previous process. Wet polishing on three 8-inch Buehler metallurgical

polishing wheels followed. Wheel one was covered with canvas. Rotating the sample 90° from the previous sanding direction, and using 500 grit carborundum, all previous marks were removed. Visually, the surface had the appearance of an old mirror with many scratches showing. The second wheel, covered with felt-like material (Kitten Ear), was used with a one micron alumina heterogeneous solution. The final wheel was covered with a softer velvet-like material (Reyvel). The abrasive used with this wheel was $\frac{1}{2}$ micron gamma alumina and produced a fine mirror finish with no visible scratches. After polishing with each wheel, the test surface was washed using a tap water jet. In addition, upon completion of polishing with the third wheel, the surface was flushed with methanol to prevent spotting, then rotated under a hot air jet, drying the surface completely. Scotch Protective Tape, Type 343, with a low adhesive coefficient was placed on the surface to protect it from scratching and oxidation during installation.

(2) Grease Coated Finish. A clean, mirror finished surface (as outlined above) was coated with Apiezon "N" vacuum grease by applying a small amount over the entire surface with a cotton swab. Small ridges were visible, however. Application of a hot air jet melted the grease to a thin, evenly distributed layer of estimated .002 inches thickness. A clear, undistorted reflection could be seen in the surface upon cooling.

(3) Oxidized Finish. A clean, mirror finished surface was oxidized by exposing it to heat. A propane torch, at about 200 - 230°F, was used to apply the heat until an opaque film covered the surface. Despite this treatment, the test surface's appearance was still smooth, and a reflection could be observed.

(4) Roughened Finish. A clean, mirror finished surface was again used as the basic surface to modify. Light taps from a small peening hammer were used on $\frac{1}{2}$ grit flint paper which covered the surface. These nucleation cavities were evenly distributed over the entire surface. The surface was then swabbed with reagent-grade methanol and dried. The maximum cavity size was approximately .003 inches diameter.

(5) Teflon-Coated Roughened Finish. After having boiled off the roughened surface, it was cleaned and one coat of green DuPont 851-204 Teflon finish was brushed on. This was wiped into the cavities using a soft paper towel. A second coat was immediately applied and wiped off, apparently filling all nucleating sites. The Teflon was then cured at a temperature of approximately 390 to 420°F by using a hot air jet for ten minutes. A slight change in hue indicated that the curing temperature had been attained.

Upon cooling, the surface was polished for one minute, smoothing out any major asperities in the Teflon. The surface was tested for and found to be non-wetting for water. A practice surface treated similarly, however, was found to be wetted by liquid nitrogen. The maximum diameter of the filled cavities was approximately .003 inches, determined by the use of a metallurgical specimen microscope. Areas between the Teflon-filled cavities were highly polished.

Testing Procedure

Each thermocouple was inserted into its respective hole with the Apiezon "N" grease, wrapped a half-turn around the boiler plate at the same distance from the boiler surface, then secured with Teflon strips. The heater power wires were attached, insulated, and fastened, using the wire itself, to the transition section to prevent breakage. Following, the wired boiler test section was pushed without difficulty, into the

enclosure with a twisting motion to coil the wires. The upper lip of the diaphragm was then soldered to the enclosure with Eutecrod 157 (Figure 6).

Upon completion of the above assembly of the boiler test plate and enclosure, the system was electrically re-checked for continuity. The boiler insulating vacuum system was connected and pump-down commenced. The boiler test surface was repolished just prior to a test run with a portable, number three wheel using gamma alumina to remove light tape marks, recleaned with tap water, flushed with methanol, then dried under a hot air jet. A small amount of Apiezon "N" grease was placed around the test surface-stainless steel interface with a hypodermic needle to reduce "rogue" nucleation sites (Figure 6). The test dewar was then hung in place, connected through the quick-disconnect seal to the vacuum system and evacuation began. A plexiglass view port was placed on its O-ring located in the flange, and evacuation began inside the dewar. This provided an easy way to rid the dewar of moisture from a previous run and, at the same time, outgas the system. Thermal system pump-down time to 2×10^{-5}mm Hg was approximately one hour. During this time, the thermal radiation barrier dewar was cleaned and put in place with unsilvered strips aligned.

Upon reaching 2×10^{-5}mm Hg, the test dewar was vented and a small quantity of liquid nitrogen was admitted to cool down the test specimen and dewar wall. Afterward, a small amount was admitted to the outer dewar. Subsequently, both dewars were filled slowly in order to prevent thermal shocks.

The heater was then energized to a heat flux of 5-6 watts/cm^2 and boiling commenced for ten minutes in order to degas the liquid nitrogen charge. The boiler was then allowed to cool. When most of the cavities had ceased nucleating, a quick vacuum, using the environmental pump, was

pulled momentarily to cause violent boiling by lowering T_s. By resuming atmospheric pressure conditions, the pressure increased thereby collapsing the remaining active nucleation sites. A waiting period followed, during which thermal equilibrium was established. This was determined by monitoring the boiler and bulk fluid thermocouples for steady readings.

The barometric pressure and ambient temperature were read prior to a run for saturation temperature correction.

A data collection run consisted of applying power at approximately 10 watt intervals up to a maximum of 82.5 watts, which corresponded to a heat flux of 16.5 watts/cm^2, and then decreasing the power at different intervals. Change in nitrogen height was recorded in order to determine the change in saturation temperature. Temperature emfs were recorded for the four thermocouples after changing heater power and waiting for thermal equilibrium to be re-established. In all cases, the thermocouple closest to the surface was re-read in order to duplicate the original reading within 1μV before changing the flux level. Approximate waiting time for equilibrium after a power change was two minutes. Thermocouple response to a step change was on the order of one second, while the response of the rest of the temperature sensing system was considerably shorter, depending on scaling time by the digital voltmeter. Usual time for taking thermocouple readings was thirty seconds at any specified heat flux.

The system was shut down by de-energizing the heater, removing the outer dewar, and disconnecting the thermal vacuum. The test dewar was removed, allowing the boiler assembly to then warm to room temperature by natural convection. The thermal insulation vacuum was maintained to the boiler/boiler enclosure during warm-up to remove any cryopumped vapors in the boiler enclosure and support tube. During operation, this cryopumping effect helped the vacuum system such that by the end of a run,

system vacuum was 6×10^{-6} mm Hg.

Treatment of Data

At any level of heat flux the emf values in microvolts were zero corrected, then converted to temperature using the working curves generated for each thermocouple. These temperatures were plotted versus boiler plate axial thermocouple position to obtain a temperature distribution. A straight line always resulted. Using the slope of this line and an average thermal conductivity (Figures 10 and 11), heat flux could be calculated directly, using the Fourier heat conduction equation: $Q/A = k_w \partial T/\partial X$. The wall temperature was determined by extrapolating the straight line temperature distribution to the boiler surface.

Saturation temperature was determined from the corrected barometric pressure and working fluid height, using the Clausius Clapeyron equation. A sample calculation is given in Appendix C.

Generally, data was processed in the metric system, as most cryogenic investigations make use of this system.

SECTION 4

RESULTS AND DISCUSSION

Six surfaces were evaluated. Heat fluxes as high as 16.5 watts/cm^2 were attained without complications. Some difficulty was encountered from "rogue" sites between the boiler interface and stainless diaphragm as they tended to obscure the boiler surface, preventing photographic records, but the mechanism of active sites spreading on the test surface was observed and estimates of nucleation coverage could be made. The Apiexon "N" grease applied, after a preliminary test, at the interface reduced the problem considerably. The effect is considered minor, as the temperature distribution was linear over the four thermocouples. Any heat flux distortion would have been reflected in the reading of the thermocouple closest to the surface.

A comparative summary of each surface is given in Table I where ΔT equals the difference between the boiler surface temperature and the saturation temperature at liquid pressure.

TABLE I - NUCLEATE BOILING DATA SUMMARY

Surface Condition	Incipient Boiling Flux w/cm^2	ΔT	Full Surface Nucleation Flux w/cm^2	ΔT	Last Observed Nucleating Site on Decreasing Flux w/cm^2	ΔT
Mirror Copper #2	1.2	4.3	2.06	4.4	$<.4$	*
Mirror Nickel	5.8	10.3	13.3	10.4	10.4	10.3
Oxidized	1.2	4.0	4.3	5.1	$<.4$	*
Rough	.4	2.3	1.8	2.4	$<.4$	*
Teflon	.5	2.5	12.5	4.0	$<.4$	*
Grease	2.6	5.4	4.8	11.0	1.8	3.6

* Indicates very small heat flux and corresponding ΔT.

Typical data points with estimated error limits for an electrical tough pitch copper mirror surface are given in Figure 12. A curve showing the experimental results of Roubeau [20], who used a copper boiler of similar size and oriented surface, is shown for comparison. The theoretical correlations of Rohsenow and Forster-Zuber [21] are also presented for comparison. The data for full surface nucleate boiling agrees well. Note that the surface temperature remains approximately constant until full nucleation is established. The reproducibility of this surface is shown in Figure 13. Arbitrarily, mirror run #2 was chosen for all subsequent comparisons.

Effect of Roughness

Figure 14 shows, comparatively, the effects of surface roughness of the copper test sample. Roughness affected not only incipient boiling flux, but wall superheat temperature as well (see Table I). As expected increased roughness provided more nucleation sites at lower wall superheat.

The effect of the Teflon coat on the roughened surface at low heat fluxes was that of partial insulation. Since nitrogen wets the Teflon, no non-wetting interfaces occurred such as observed by Young and Hummel [26] with a water-Teflon-metal combination, which produced heat transfer coefficients ten times the plain roughened surface (Fig. 19). However, the Teflon provided areas of low free surface energy (whereas the copper had a high free surface energy [27]), altering the surface tension forces and allowing a somewhat higher heat flux for a given ΔT.

A plausible explanation of the Teflon curve crossing the rough surface curve is that, originally, a greater surface temperature was required to activate a site located on the Teflon (bubble nucleation point seen visually) due to the insulating effects of Teflon (similar to

grease coating discussed in the following section), but that, once energized, greater heat transfer could take place due to the greater number of activation points. The bubbles formed were smaller in diameter, but larger numbers of them were seen per surface area, giving an overall higher heat flux.

Effect of Contaminants

The effect of surface contaminants (Figure 15) is that of insulation requiring higher surface temperature for a given flux. This effect was expected for the oxidized surface [5] as well as the greased surface [1], but, because of an insufficiently thick layer of oxide, the boiling curve for this surface coincided with the results of the mirror finish-un-oxidized. It was not possible to re-investigate the effects of surface oxide thickness for this study.

The surface coated with Apiezon "N" grease followed expectations with increasing heat flux. Heat flux change was approximately proportional to ΔT up to 5 watts/cm^2, indicating a conduction layer. At full surface nucleation (5 watts/cm^2), the slope assumed the characteristic nucleate boiling form. Boiling, however, causes a physical change in the grease surface, discussed in greater detail in the following section.

Hysteresis Effects

The differences in observed superheat when the heat flux is increased, reduced, and again increased, is called hysteresis. This effect is vividly demonstrated in Figure 16, showing the Teflon and greased surfaces. It was also observed to a much smaller extent (not shown) in the mirror copper surface. The explanation is that for the original flux increase, a few small nucleate patches became activated. At increasingly higher heat fluxes these patches spread, activating nearby sites. Upon decreasing heater power, these active sites were observed to thin out evenly, but

many remained active at fluxes which previously had caused only convection heat transfer or partial boiling. Since the time for a data taking run was usually an hour, changes in surface entrapped vapor were expected. As the surface boiled, more noncondensable vapor was boiled off. The final effect was that more energy and consequently a higher ΔT was required to reactivate a surface as the population of any one sized fertile site (one containing vapor) had been reduced. The Teflon coated sample followed expectations. Observation of this surface showed that for a small heat flux (.4 watts/cm^2), a small area of sites was activated. With an increase in power, more of the surface was covered with nucleation sites. The number of active sites increased rather slowly. It was not until a heat flux of 12 watts/cm^2 was established that the whole surface became covered. On decreasing flux, all sites remained active, however, and at 0.4 watts/cm^2, the bubble columns were very fine, hair-like streams, indicating many active sites. At this condition, the lowest ΔT (.3°K) was recorded for nucleate boiling with any surface considered in this investigation. The reactivation wall temperature was higher, as expected.

The grease coated surface showed a wider hysteresis curve because of the aforementioned altered surface condition. This change was noted on power reduction. At each point where nucleation had occurred, a small indentation appeared in the grease. These indentations were distributed evenly over the surface. The plausible explanation is that the surface became superheated enough to transfer energy in such great quantity to the entrapped vapor on the polished surface thereby activating nucleation sites. Bubbles formed from these sites with enough force to deform and remove the grease, (which acts as a brittle solid at liquid nitrogen temperature). Differing from the Teflon surface, however, it was noted that the reactivation energy was lower than activation energy because

the surface resistance to nucleation had been decreased due to the "pits". It was intended to record this phenomenon photographically in order to provide data on the number of active sites per unit area. Upon dismantling and warming the surface to ambient temperature to get a close-up photograph, however, the grease was observed to flow partially thus diminishing the effect.

Effect of Materials

The effect of material is shown in Figure 17. The results show better heat transfer with copper than with nickel. This result agrees with Berenson's [5] results for pentane. The data for platinum [13] is also shown. The thermal conductivity of platinum is very similar to that of nickel and, as can be seen when the surface is nucleating fully, the curves are very similar.

Due to the lower thermal diffusity ($\alpha = \frac{k_w}{C_w \rho_w}$) of nickel compared to copper at LN_2 temperatures, the bubble generation rate is lower, resulting in poorer heat transfer. A plot of α versus wall superheat (Figure 18) clearly shows that as the thermal diffusivity of the boiler surface increases, the wall superheat decreases (and hence higher heat transfer coefficients).

The nickel surface was unusual in that it was the only surface investigated which exhibited a temperature drop for a heat flux increase (Figure 17). As yet, no explanation exists for this negative slope phenomenon [24]. There may exist an unstable condition, as observed by Marto [14] with sodium pool boiling. The basis for this conclusion is that the thermocouple closest to the surface was observed to flucturate $\pm$ 3μV (0.3°K overall) at 5.8 watts/cm^2, finally settling to $\pm$ 1μV at 13.3 watts/cm^2. Virtually no hysteresis occurred on power decrease, and this same unstable thermocouple fluctuation was observed

in the vicinity of 10.4 watts/cm^2 heat flux.

A general comparison covering the spectrum of materials and fluids used in heat transfer equipment is shown in Figure 19. Of interest is that, in general, the observed heat transfer coefficient is very nearly 5×10^3 BTU/(hr ft^2 °F) for all cases at the highest observed temperatures (fluxes).

SECTION 5

Conclusions with Recommendations

The results discussed lead to the following conclusions:

1. Surface conditions significantly affect the incipient boiling, the nucleate boiling wall superheat and slope of the boiling curve of liquid nitrogen.

2. Boiler history (i.e. whether previous boiling has occurred on the surface and whether the heat flux is being increased or decreased) affects the nucleate boiling wall superheat, (T_w-T_s).

3. Boiler surface materials affect the boiling curve of liquid nitrogen.

Therefore, correlating equations such as that of Rohsneow and Forster-Zuber, should be used only when all surface conditions are specified and account has been made for each variation from a reference condition.

The results indicate that further studies be continued in order to:

1. Completely eliminate all "rogue" nucleation sites on the boiler test surface.

2. Determine the effect of surface conditions on bubble frequency using a high speed motion picture camera.

3. Continue studies with heavier layers of oxide and grease to further bear out the effects of contaminants and add further credence to application of the entrapped vapor phase nucleation site theory at cryogenic temperatures [3].

4. Study the effect of wettability and non-wettability in conjunction with small sized or artificial cavities.

5. Widen the realm of cryogenic fluid heat transfer studies by using liquid helium as a working fluid and investigate the effect of surface conditions.

ACKNOWLEDGEMENT

The author wishes to thank LT Paul J. Marto, USNR, D. Sci., for his generous contributions of time and energy, and his enthusiasm in all phases of this research. The author is also indebted to Professor D. N. Lyon at the University of California (Berkeley) for discussion of his experiences and guidance in design problem areas. Grateful thanks go also to Mr. Ian van Gastel for his aid in all glasswork, Mr. August Rasmussen for his many hours in the machine shop, and to Mr. Kenneth W. Mothersell and Mr. Joseph S. Beck for their assistance in the laboratory.

BIBLIOGRAPHY

1. Averin, E.K., "The Effect of the Material and of the Mechanical Treatment of the Surface on the Heat Exchange in the Boiling of Water", Izv. A. K. Nauk, USSR, Otd. Tekh. Nauk, 3, pp. 116-122 (1954) (AERE-lib/Trans.-562).

2. Baker, H. Dean, Ryder, E. A., and Baker, N. H., Temperature Measurement in Engineering, Vol. I, New York: J. Wiley & Sons (1953).

3. Bankoff, S. G., "Ebullition from Solid Surfaces in the Absence of a Pre-Existing Gaseous Phase", Trans. ASME (May, 1957), Jnl. of Heat Transfer, 79, p. 735 (1957).

4. Berenson, P. J., "Experiments on Pool Boiling Heat Transfer", Int'l Jnl. of Heat and Mass Transfer, 5, October (1962).

5. _____, "Transition Boiling Heat Transfer from a Horizontal Surface", Technical Report 17, MIT DSR Prog. 7-8077.

6. Bonilla, C. F., Weiner, M. M., and Bilfinger, H., "Pool Boiling of Potassium", Proceedings of the High-Temperature Liquid-Metal Heat Transfer Technology Meeting, 1, p. 291 (1963).

7. Brentari, E. G., Giarratano, P. J. and Smith, R. V., "Boiling Heat Transfer for Oxygen, Nitrogen, Hydrogen, and Helium", NBS Technical Note 317, September (1965).

8. Corty, C. and Foust, A. S., "Surface Variables in Nucleate Boiling", A. I. Ch. E. Heat Transfer Conference, St. Louis, Mo. (1953).

9. Dike, P. H., Thermoelectric Thermometry, Philadelphia: Leeds and Northrup Company (1954).

10. Griffith, P. and Wallis, J. D., "The Role of Surface Conditions in Nucleate Boiling", ASME-A. I. Ch. E. Heat Transfer Conference, Storrs, Conn. (1959).

11. Hodgman, C. D. (Ed), Handbook of Chemistry and Physics, Cleveland, Ohio: Chemical Rubber Co. (1946).

12. Johnson, V. J. (Ed.), "A Compendium of the Properties of Materials at Low Temperature" (Phase II), December (1961).

13. Koskey, P. G. and Lyon, D. N., Department of Chemical Engineering, University of California, Berkeley, Private Correspondence (1966).

14. Marto, P. J. and Rohsenow, W. M., "The Effect of Surface Conditions on Nucleate Pool Boiling Heat Transfer to Sodium", D. Sci. Thesis, Massachusetts Institute of Technology (1965), (AEC Code: Report MIT-3357-1).

15. Morrison, R., "Shielding Signal Circuits", ISA Jnl., 13, p. 58, March (1966).

16. Powell, R.L. and Sparks, L. L., "Available Low Temperature Thermocouple Information and Services", NBS Report 8750, February, (1965).

17. _____, Caywood, L. P. Jr., Bunch, M. D., "Low Temperature Thermocouples", Temperature, Its Measurement and Control in Science and Industry, Vol. 3, Part 2, A. I. Dahl (ed), New York: Reinhold Publishing Corporation (1962).

18. Reese, W., Anderson, A. C. and Wheatley, J. C., "Thermal Conductivity of Some Amorphous Dielectric Solids Below 1°K", Rev. of Sci. Inst., 34, p. 1386-1390, December (1963).

19. Rohsenow, W. M., "A Method of Correlating Heat -Transfer Data for Surface Boiling of Liquids", Trans. ASME, 74, p. 969, August (1952).

20. Roubeau, P., "Echanges Thermiques dans L'Asote et L'Hydragene Bouillant sous Pression", Progress in Refrigeration Science and Technology, Vol. I, Pergammon Press (1960).

21. Seader, J. D., Miller, W. S. and Kalvinskas, L. A., Boiling Heat Transfer for Cryogenics, Rocketdyne R-5598, May (1964).

22. Scott, R. B., Cryogenic Engineering, New York: D. Van Nostrand Company, Inc., (1963).

23. Westwater, J. W., Clark, H. B and Strenge, P. S., "Active Sites for Nucleate Boiling", A. I Ch. E. Heat Transfer Conference, Chicago, Ill. (1959).

24. Westwater, J. W., "Things we Don't Know about Boiling Heat Transfer", Research in Heat Transfer, Pergammon Press (1963).

25. White, G. K., Experimental Techniques in Low-Temperature Physics, Oxford: The Clarendon Press (1959).

26. Young, R. K. and Hummel, R. L., "Improved Nucleate Boiling Heat Transfer", Chemical Engineering Progress, 60, p. 53, July (1964).

27. Ziegler, W. T., Mullins, J. C., "Calculation of the Vapor Pressure and Heats of Vaporization and Sublimation of Liquids and Solids, expecially Below One Atmosphere, IV. Nitrogen and Flourine", NBS Contract CST-7404, April (1963).

28. Zisman, W. A., "Relation of Chemical Constitution to the Wetting and Spreading of Liquids on Solids", (Presented at Office of Naval Research Decennial Symposium, Washington, D.C., March 19,1957).

APPENDIX A

Calibration

Because a high degree of accuracy was desired, direct instrument calibration against secondary standards was chosen as the best means to attain the results. The amplifier-voltmeter combination was set up in an electonically noise-free room, using regulated power in order to reduce electronic disturbances. A standard cell of 1.01944 volts was used in combination with a voltage divider to generate small signals (0-600 μV). The amplifier was then adjusted so that the output displayed on the digital voltmeter agreed with the value determined by a Rubicon potentiometer known to be accurate to within 5 μV. Periodically, for the next three days, amplifier drift was checked. It was determined to be less than 1 μV. No change was observed using unregulated power. A month later, calibration was re-checked against a Leeds and Northrup K-3 Guarded Precision Potentiometer. The amplifier-digital voltmeter combination agreed to $\pm$ 1 μV over the 0-600 μV. The accuracy of the K-3 potentiometer is $\frac{1}{2}$ μV.

Using techniques outlined by the National Bureau of Standards [17], the thermocouples were checked for homogeneity after installation. Due to the limited range over which the thermocouples were to be used, calibration was accomplished by using two known boiling points covering the temperature spectrum of expected data points. In each case, the reference used was liquid nitrogen. Aviator's liquified oxygen (99.95% purity) was used as the prime calibrating point. Data was recorded for the LN_2-LN_2 combination prior to LN_2- LOX. The small zero readings were subtracted from the liquid oxygen reading for each T. C. The known boiling points were corrected (method in Appendix C) to standard pressure (760. mm Hg).

The LOX boiling point was extremely stable. Generated emfs remained within $\pm$ 1 μV over a half hour period and were reproducible on a succeeding day.

This data then became the input to a computer program developed by the NBS Cryogenic Laboratories at Boulder, Colorado [16]. The program, described fully in Appendix C, compared the resultant spot calibration with the NBS calibration table, calculated a correction factor, then generated a working table for each thermocouple. An option was built into the program so that the printed output tabulation of temperature, emf and slope was based on a liquid nitrogen reference. An example of the output is presented in Appendix C also.

In order to check the accuracy, the boiling point of liquid methane was used as a check. Ultra pure methane (99.95%) was liquified in the laboratories. For an as yet unexplained reason, the temperature of the LCH_4 decreased with time. It was assumed that the LCH_4 was undergoing a contamination with the atmosphere. Notwithstanding, an emf-time graph was drawn for each thermocouple tested over a period of six minutes, and the subsequent straight line was extrapolated to a zero time value (completion of liquification). The time between liquification and first datum point was 30 seconds. This temperature decay with time was observed each time the methane was liquified. The extrapolated values were used to generate working tables for each thermocouple. The methane tables were compared with the oxygen-based tables and agreed within 3.4 μV (.16°K) at liquid methane temperature (111.6°K).

A summary of both generated working tables at several arbitrary temperatures appears in Table A-1.

TABLE A-1

WORKING THERMOCOUPLE TABLE SUMMARY

Temp. °K	T.C.	LOX μV	LCH_4 μV	Difference LOX-LCH_4 μV	Diff. °K
	1	43.6	43.5	.1	.006
	2	43.8	43.6	.2	.012
80	3	44.0	43.7	.1	.006
	4	43.8	43.7	.1	.006
	5	43.8	43.6	.2	.012
	1	216.3	216.1	.2	.011
	2	217.3	216.6	.7	.039
90	3	218.3	217.1	1.2	.067
	4	217.3	217.1	.2	.011
	5	217.3	216.6	.7	.039
	1	402.3	401.9	.4	.021
	2	404.1	402.7	1.4	.073
100	3	406.0	403.7	2.3	.119
	4	404.1	403.7	.4	.021
	5	404.1	402.9	1.2	.062
	1	601.2	600.6	.6	.029
	2	603.9	601.8	2.1	.102
110	3	606.7	603.3	3.4	.165
	4	603.9	603.3	.6	.029
	5	603.9	602.0	1.9	.093

APPENDIX B

Generation of Thermocouple Tables

Working thermocouple tables were generated using guidelines set forth in NBS 8750 [16] and program FACTOR with standard copper-constantan (TP-TN) thermocouple table decks. This program with tables was available at cost from NBS Cryogenic Laboratories, Boulder Colorado. It was written in FORTRAN II, but modified by the author to conform to FORTRAN 60 for submission to U.S. Naval Postgraduate School Computer Facility using CDC 1604. This modified version of the program is presented along with the standard table and input data at the end of this appendix. In addition, selected cards were pulled from the program deck and collected together in a manner suitable for checking spacing of card information and commands. Finally, an example of a generated working table has been included.

The computer compares the observed temperature change in degrees and μV with the standard table values and calculates a factor from this ratio (μV measured/μV standard). A table is then printed from 0 to 300°K for any selected reference temperature in this range.

Input data to the program appears on two or more cards depending on how many different tables are being processed sequentially on the one program submission. Card A contains calibration information, the details of which are as follows:

Column 1-6: Temperature scale; either DEG. K or DEG. C. Units must be consistent throughout this card. The space between the period and K or C is required.

Column 11-20: High Temperature of spot calibration which must include a decimal point.

Column 21-30: Low temperature of spot calibration with decimal point.

Column 31-40: Voltage difference observed from spot calibration in microvolts with decimal point.

Column 41-50: Reference temperature desired for tables with decimal point.

Column 58-60: Punch YES if punched cards desired with table-- otherwise punch NO in columns 58-59.

Card B is used as an identification card, the details of which are as follows:

Column 1-15: Company or laboratory identification

Column 21-26: Six characteristics available for lot number, or spool identification.

Column 31-42: User's name.

Column 51-64: Date of test.

Card C is used as a repeat card and must preceed subsequent to A and B cards for multiple table output. It should be exactly as follows in all cases:

Column 1-21: Punch REPEAT LAST T. C. DECK.

Column 50: Punch 0 (Zero).

Column 55-60: Punch DEG. K with space between period and K. Use DEG. K regardless of units wanted.

Column 68-70: Punch YES.

Assembly of the deck for submission to the computer from top to bottom was;

a. Computer monitor control cards

b. FACTOR program deck

c. Standard data deck

d. Card A

e. Card B

f. Repeat card

g. Card A

h. Card B

i. Repeat card

j. etc.....

} Multiple table output

Computer run time for programing 18 sets of data was two and one-half minutes.

REF. [16]

```
      PROGRAM FACTOR
CFCTOR  ADJUSTMENT OF PUBLISHED TABLES FOR UNITS,REF. TEMPS,AND FACTOR
   90 DIMENSION T(300),IT(300),TOC(300),EMFIN(300),EMF(300),DELEM(300),
   901DEDTIN(300),DEDT(300)
   10 FORMAT(A6,4X,4F10.0,7X,A3)
   11 FORMAT(49X,I1,4X,A6,7X,A3)
   12 FORMAT(A6,A6,A3,5X,A6,4X,A6,A6,8X,A6,A6,A2)
   13 FORMAT(A6,A4,F10.0,F10.2,F10.3,10X,F10.0,F10.2,F10.3)
   14 FORMAT(10X,3I10,4A6,A2)
   16 FORMAT(2(10X,3F10.0))
   30 FORMAT(3X,4HTEMP,5X,3HEMF,3X,6HDELEMF,5X,5HDE/DT,7X,4HTEMP,5X,
   3013HEMF,3X,6HDELEMF,5X,5HDE/DT,3X)
   40 FORMAT(2X,5HDEG K,4X,5HMIC V,2X,5HMIC V,4X,9HMIC V/DGK,4X,5HDEG K,
   4014X,5HMIC V,2X,5HMIC V,4X,9HMIC V/DGK//)
   41 FORMAT(2X,5HDEG C,4X,5HMIC V,2X,5HMIC V,4X,9HMIC V/DGC,4X,5HDEG C,
   4114X,5HMIC V,2X,5HMIC V,4X,9HMIC V/DGC//)
   50 FORMAT(I7,F10.2,F7.2,F10.3,I11,F10.1,F7.1,F10.3//)
   55 FORMAT(I7,F10.2,F7.2,F10.3,I11,F10.1,F7.1,F10.3)
   60 FORMAT(I7,F9.1,F7.1,F11.3,I11,F10.1,F7.1,F10.3//)
   65 FORMAT(I7,F9.1,F7.1,F11.3,I11,F10.1,F7.1,F10.3)
   70 FORMAT(I7,F9.1,F7.1,F11.3//)
   80 FORMAT(1H1,24H THERMOCOUPLE TABLE FOR ,A6,4H VS ,A6,11H, ISA TYPE
   801,A6,A2,10H, BASED ON/29H NAT. BUR. OF STANDARDS PUB. ,A6,28H WITH
   802CALC. MULT. FACTOR OF ,F7.5,1H./1X,A6,A6,A3,6H, LOT ,A6,29H. USERS
   803 REFERENCE TEMPERATURE,F7.3,1X,A6/16X,10HTEST DATE ,A6,A6,A2,5H  B
   804Y ,A6,A6//)
C
C      DATA DECK AND KEY CARDS READ IN
  100 READ INPUT TAPE 5,11,IA,ATEST1,ATEST2
```

```
  102 IF(IA)140,140,105
  105 READ INPUT TAPE 5,14,ITEMPI,ITABLE,IFMTCH,AMATP,AMATN,APUB,
 1051         ATYPE1,ATYPE2
  110 K2=IFMTCH+1
  112 ITEMPL=ITABLE
  115 DO 130 I=ITEMPI,ITEMPL,2
  120 READ INPUT TAPE 5,16,T(I),EMFIN(I),DEDTIN(I),T(I+1),EMFIN(I+1),
 1201DEDTIN(I+1)
  130 CONTINUE
  132 K9=K2
  133 IF(IFMTCH)134,134,140
  134 K9=K2+1
  140 READ INPUT TAPE 5,10,AUNIT,TEMPHI,TEMPLO,ETEST,UREFT,ACARD
  141 ITABLE=ITEMPL
  142 IUNIT=1
  144 REFTMP=UREFT
  150 READ INPUT TAPE 5,12,ACOMP1,ACOMP2,ACOMP3,ALOT,ANAMEI,ANAMEL,
 1501ADATE1,ADATE2,ADATE3
C
C     CONVERSION OF REFTMP,TEMPHI, AND TEMPLO INTO DEG. K SYSTEM
  151 IF(AUNIT-ATEST1)152,155,152
  152 REFTMP=REFTMP+273.15
 1152 TEMPHI=TEMPHI+273.15
 2152 TEMPLO=TEMPLO+273.15
 3152 IUNIT=2
C
C     COMPUTATION OF FACTOR
```

```
  155 ITEMLO=TEMPLO
  160 TEMP3=ITEMLO-1
  165 TEMP4=ITEMLO
  170 TEMP5=ITEMLO+1
  175 EMFI3=EMFIN(ITEMLO-1)
  180 EMFI4=EMFIN(ITEMLO)
  185 EMFI5=EMFIN(ITEMLO+1)
  190 U=EMFI3*(TEMPLO-TEMP4)*(TEMPLO-TEMP5)/2.0
  195 V=EMFI4*(TEMPLO-TEMP3)*(TEMP5-TEMPLO)
  200 W=EMFI5*(TEMPLO-TEMP3)*(TEMPLO-TEMP4)/2.0
  205 EMFLO=U+V+W
  210 ITEMHI=TEMPHI
  215 TEMP6=ITEMHI-1
  220 TEMP7=ITEMHI
  225 TEMP8=ITEMHI+1
  230 EMFI6=EMFIN(ITEMHI-1)
  235 EMFI7=EMFIN(ITEMHI)
  240 EMFI8=EMFIN(ITEMHI+1)
  245 X=EMFI6*(TEMPHI-TEMP7)*(TEMPHI-TEMP8)/2.0
  250 Y=EMFI7*(TEMPHI-TEMP6)*(TEMP8-TEMPHI)
  255 Z=EMFI8*(TEMPHI-TEMP6)*(TEMPHI-TEMP7)/2.0
  260 EMFHI=X+Y+Z
  265 ETABLE=EMFHI-EMFLO
  270 FACTOR=ETEST/ETABLE
C
C       CALCULATION OF EMFR
  305 IF(REFTMP)320,310,320
  310 EMFR=0.0
  315 GO TO 375
```

```
  320 ITEMP0=REFTMP
  325 TEMP0=ITEMP0
  330 TEMP1=TEMP0+1.0
  335 TEMP2=TEMP0+2.0
  340 EMFI0=EMFIN(ITEMP0)
  345 EMFI1=EMFIN(ITEMP0+1)
  350 EMFI2=EMFIN(ITEMP0+2)
  355 A=EMFI0*(REFTMP-TEMP1)*(REFTMP-TEMP2)/2.0
  360 B=EMFI1*(REFTMP-TEMP0)*(TEMP2-REFTMP)
  365 C=EMFI2*(REFTMP-TEMP0)*(REFTMP-TEMP1)/2.0
  372 EMFR=(A+B+C)*FACTOR
  374 IF(IUNIT-1)465,375,465
C
C     CALCULATION OF EMF AND DEDT FOR ENTIRE TEMP. RANGE
  375 DO 395 J=ITEMPI,ITEMPL
  380 IT(J)=T(J)
  385 EMF(J)=EMFIN(J)*FACTOR-EMFR
  390 DEDT(J)=DEDTIN(J)*FACTOR
  395 CONTINUE
  396 GO TO 398
C
C     EMF,DELEMF,AND DEDT VALUES CORRESPONDING TO EVEN DEG. C
  465 K3=ITEMPL-2
  470 DO 540 I=ITEMPI,K3
  480 D=EMFIN(I)*0.78625
  485 E=EMFIN(I+1)*0.27750
  490 F=EMFIN(I+2)*(-0.06375)
```

```
  495 EMF(I)=(D+E+F)*FACTOR-EMFR
  500 X=DEDTIN(I)*0.78625
  505 Y=DEDTIN(I+1)*0.27750
  510 Z=DEDTIN(I+2)*(-0.06375)
  515 DEDT(I)=(X+Y+Z)*FACTOR
  540 CONTINUE
  545 K4=K3+1
  560 D1=EMFIN(K4-1)*(-0.06375)
  565 E1=EMFIN(K4)*0.97750
  570 F1=EMFIN(K4+1)*0.08625
  575 EMF(K4)=(D1+E1+F1)*FACTOR-EMFR
  580 X1=DEDTIN(K4-1)*(-0.06375)
  585 Y1=DEDTIN(K4)*0.97750
  590 Z1=DEDTIN(K4+1)*0.08625
  595 DEDT(K4)=(X1+Y1+Z1)*FACTOR
  620 ITABLE=ITABLE-1
  625 DO 635 I=ITEMPI,273
  630 IT(I)=T(I)-273.15
  635 CONTINUE
  640 DO 650 I=274,ITABLE
  645 IT(I)=T(I)-272.85
  650 CONTINUE
C
C     CALCULATION OF DELEMF
  398 DELEM(1)=EMF(1)+EMFR
  399 L1=ITEMPI+1
  400 DO 420 J=L1,IFMTCH
  405 E2=EMF(J)+0.005
  410 E3=EMF(J-1)+0.005
```

```
  415 DELEM(J)=EMF(J)-EMF(J-1)-MODF(E2,0.01)+MODF(E3,0.01)
  420 CONTINUE
  425 DO 445 J=K9,ITABLE
  430 E4=EMF(J)+0.05
  435 E5=EMF(J-1)+0.05
  440 DELEM(J)=EMF(J)-EMF(J-1)-MODF(E4,0.1)+MODF(E5,0.1)
  445 CONTINUE
C
C     PAGE HEADING WRITEOUT
  665 WRITE OUTPUT TAPE 6,80,AMATP,AMATN,ATYPE1,ATYPE2,APUB,FACTOR,
 6651ACOMP1,ACOMP2,ACOMP3,ALOT,UREFT,AUNIT,ADATE1,ADATE2,ADATE3,
 6652ANAMEI,ANAMEL
  680 WRITE OUTPUT TAPE 6,30
  685 GO TO (690,700),IUNIT
  690 WRITE OUTPUT TAPE 6,40
  695 GO TO 704
  700 WRITE OUTPUT TAPE 6,41
C
C     WRITEOUT FOR PARAMETERS FROM T=1 TO T=FORMAT CHANGE
  704 IF(IFMTCH)780,780,705
  705 DO 775 L=ITEMPI,IFMTCH
  710 IF(XMODF(L-ITEMPI+1,5))735,715,735
  715 IF(XMODF(L-ITEMPI+1,40))735,735,725
  725 WRITE OUTPUT TAPE 6,50,IT(L),EMF(L),DELEM(L),DEDT(L),IT(L+40),
 7251EMF(L+40),DELEM(L+40),DEDT(L+40)
  730 GO TO 775
  735 WRITE OUTPUT TAPE 6,55,IT(L),EMF(L),DELEM(L),DEDT(L),IT(L+40),
```

```
     7351EMF(L+40),DELEM(L+40),DEDT(L+40)
     775 CONTINUE
C
C        WRITE OUT FOR PARAMETERS FROM T=FORMAT CHANGE TO T=40
     780 DO 850 L=K2,40
     785 IF(XMODF(L-ITEMPI+1,5))810,790,810
     790 IF(XMODF(L-ITEMPI+1,40))810,810,800
     800 WRITE OUTPUT TAPE 6,60,IT(L),EMF(L),DELEM(L),DEDT(L),IT(L+40),
     8001EMF(L+40),DELEM(L+40),DEDT(L+40)
     805 GO TO 850
     810 WRITE OUTPUT TAPE 6,65,IT(L),EMF(L),DELEM(L),DEDT(L),IT(L+40),
     8101EMF(L+40),DELEM(L+40),DEDT(L+40)
     850 CONTINUE
     855 N=0
C
C        PAGE HEADING WRITE OUT
     865 WRITE OUTPUT TAPE 6,80,AMATP,AMATN,ATYPE1,ATYPE2,APUB,FACTOR,
     8651ACOMP1,ACOMP2,ACOMP3,ALOT,UREFT,AUNIT,ADATE1,ADATE2,ADATE3,
     8652ANAMEI,ANAMEL
     870 WRITE OUTPUT TAPE 6,30
     875 GO TO (880,890),IUNIT
     880 WRITE OUTPUT TAPE 6,40
     885 GO TO 900
     890 WRITE OUTPUT TAPE 6,41
C
C        PARAMETER WRITE OUT FOR SECOND,THIRD,ETC. PAGES
     900 N=N+1
     905 J=80*N+1
     906 JE=J+39
```

```
  910 DO 1065 L=J,JE
  930 IF(L-ITABLE)935,935,1075
  935 IF(L+40-ITABLE)940,940,1005
  940 IF(XMODF(L-ITEMPI+1,5))965,945,965
  945 IF(XMODF(L-ITEMPI+1,40))965,965,955
  955 WRITE OUTPUT TAPE 6,60,IT(L),EMF(L),DELEM(L),DEDT(L),IT(L+40),
 9551EMF(L+40),DELEM(L+40),DEDT(L+40)
  960 GO TO 1065
  965 WRITE OUTPUT TAPE 6,65,IT(L),EMF(L),DELEM(L),DEDT(L),IT(L+40),
 9651EMF(L+40),DELEM(L+40),DEDT(L+40)
  970 GO TO 1065
 1005 IF(XMODF(L-ITEMPI+1,5))1030,1010,1030
 1010 IF(XMODF(L-ITEMPI+1,40))1030,1030,1020
 1020 WRITE OUTPUT TAPE 6,70,IT(L),EMF(L),DELEM(L),DEDT(L)
 1025 GO TO 1065
 1030 WRITE OUTPUT TAPE 6,65,IT(L),EMF(L),DELEM(L),DEDT(L)
 1065 CONTINUE
 1070 IF(J+79-ITABLE)865,1075,1075
C
C      PUNCHED DECK OUTPUT
 1075 IF(ACARD-ATEST2)1200,1080,1200
 1080 DO 1100 I=ITEMPI,ITABLE,2
 1085 TOC(I)=IT(I)
 1090 TOC(I+1)=IT(I+1)
 1091 IF(I-ITABLE)1095,1097,1097
 1095 WRITE OUTPUT TAPE 7,13,AMATP,AMATN,TOC(I),EMF(I),DEDT(I),TOC(I+1),
 10951EMF(I+1),DEDT(I+1)
 1096 GO TO 1100
```

```
 1097 WRITE OUTPUT TAPE 7,13,AMATP,AMATN,TOC(I),EMF(I),DEDT(I)
 1100 CONTINUE
 1200 GO TO 100
      END
      END
```

```
KEY CARD 1                                          1    DEG. K        YES
KEY CARD 2          1        300      26COPPERCONST.R-188 TP-TN
TP VS TN           1.       0.17     0.331                2.       0.66      0.657
TP VS TN           3.       1.48     0.978                4.       2.62      1.295
TP VS TN           5.       4.07     1.607                6.       5.83      1.914
TP VS TN           7.       7.90     2.217                8.      10.27      2.515
TP VS TN           9.      12.93     2.808               10.      15.88      3.096
TP VS TN          11.      19.12     3.380               12.      22.64      3.659
TP VS TN          13.      26.43     3.933               14.      30.50      4.203
TP VS TN          15.      34.83     4.468               16.      39.43      4.731
TP VS TN          17.      44.29     4.992               18.      49.41      5.251
TP VS TN          19.      54.78     5.509               20.      60.41      5.765
TP VS TN          21.      66.29     6.018               22.      72.42      6.268
TP VS TN          23.      78.80     6.516               24.      85.43      6.761
TP VS TN          25.      92.31     7.003               26.      99.43      7.242
TP VS TN          27.     106.80     7.478               28.     114.40      7.711
TP VS TN          29.     122.20     7.942               30.     130.30      8.170
TP VS TN          31.     138.60     8.395               32.     147.10      8.617
TP VS TN          33.     155.80     8.837               34.     164.70      9.054
TP VS TN          35.     173.90     9.269               36.     183.30      9.481
```

TP VS TN	37.	192.90	9.691	38.	202.70	9.898
TP VS TN	39.	212.70	10.103	40.	222.90	10.305
TP VS TN	41.	233.30	10.505	42.	243.90	10.703
TP VS TN	43.	254.70	10.898	44.	265.70	11.091
TP VS TN	45.	276.80	11.282	46.	288.20	11.470
TP VS TN	47.	299.80	11.656	48.	311.60	11.840
TP VS TN	49.	323.50	12.022	50.	335.60	12.202
TP VS TN	51.	347.90	12.380	52.	360.40	12.555
TP VS TN	53.	373.00	12.728	54.	385.80	12.899
TP VS TN	55.	398.80	13.068	56.	411.90	13.236
TP VS TN	57.	425.20	13.402	58.	438.70	13.565
TP VS TN	59.	452.40	13.726	60.	466.20	13.885
TP VS TN	61.	480.10	14.043	62.	494.20	14.199
TP VS TN	63.	508.50	14.353	64.	522.90	14.505
TP VS TN	65.	537.50	14.655	66.	552.30	14.804
TP VS TN	67.	567.20	14.951	68.	582.20	15.096
TP VS TN	69.	597.30	15.239	70.	612.60	15.380
TP VS TN	71.	628.10	15.518	72.	643.70	15.653
TP VS TN	73.	659.40	15.786	74.	675.20	15.918
TP VS TN	75.	691.20	16.050	76.	707.30	16.182
TP VS TN	77.	723.50	16.314	78.	739.90	16.447
TP VS TN	79.	756.40	16.580	80.	773.00	16.713
TP VS TN	81.	789.70	16.846	82.	806.60	16.979
TP VS TN	83.	823.60	17.112	84.	840.80	17.245
TP VS TN	85.	858.10	17.378	86.	875.50	17.511
TP VS TN	87.	893.10	17.644	88.	910.80	17.777
TP VS TN	89.	928.70	17.910	90.	946.70	18.043
TP VS TN	91.	964.80	18.176	92.	983.00	18.309
TP VS TN	93.	1001.40	18.441	94.	1019.90	18.573

TP VS TN	95.	1038.50	18.705	96.	1057.30	18.836
TP VS TN	97.	1076.20	18.967	98.	1095.20	19.097
TP VS TN	99.	1114.40	19.227	100.	1133.70	19.357
TP VS TN	101.	1153.10	19.486	102.	1172.70	19.615
TP VS TN	103.	1192.40	19.744	104.	1212.20	19.873
TP VS TN	105.	1232.10	20.001	106.	1252.20	20.129
TP VS TN	107.	1272.40	20.257	108.	1292.70	20.384
TP VS TN	109.	1313.10	20.511	110.	1333.70	20.638
TP VS TN	111.	1354.40	20.765	112.	1375.20	20.892
TP VS TN	113.	1396.20	21.019	114.	1417.30	21.146
TP VS TN	115.	1438.50	21.272	116.	1459.80	21.398
TP VS TN	117.	1481.30	21.524	118.	1502.90	21.650
TP VS TN	119.	1524.60	21.775	120.	1546.40	21.901
TP VS TN	121.	1568.40	22.027	122.	1590.50	22.153
TP VS TN	123.	1612.70	22.279	124.	1635.00	22.405
TP VS TN	125.	1657.50	22.530	126.	1680.10	22.655
TP VS TN	127.	1702.80	22.780	128.	1725.60	22.905
TP VS TN	129.	1748.60	23.030	130.	1771.70	23.155
TP VS TN	131.	1794.90	23.281	132.	1818.30	23.407
TP VS TN	133.	1841.80	23.533	134.	1865.40	23.659
TP VS TN	135.	1889.10	23.784	136.	1912.90	23.910
TP VS TN	137.	1936.90	24.036	138.	1961.00	24.162
TP VS TN	139.	1985.20	24.288	140.	2009.50	24.414
TP VS TN	141.	2034.00	24.540	142.	2058.60	24.666
TP VS TN	143.	2083.30	24.793	144.	2108.20	24.919
TP VS TN	145.	2133.20	25.045	146.	2158.30	25.170
TP VS TN	147.	2183.50	25.294	148.	2208.90	25.417
TP VS TN	149.	2234.40	25.540	150.	2260.00	25.663
TP VS TN	151.	2285.70	25.785	152.	2311.60	25.907

TP VS TN	153.	2337.60	26.028	154.	2363.70	26.148
TP VS TN	155.	2389.90	26.268	156.	2416.20	26.388
TP VS TN	157.	2442.60	26.507	158.	2469.20	26.625
TP VS TN	159.	2495.90	26.743	160.	2522.70	26.860
TP VS TN	161.	2549.60	26.977	162.	2576.60	27.094
TP VS TN	163.	2603.80	27.211	164.	2631.10	27.327
TP VS TN	165.	2658.50	27.443	166.	2686.00	27.559
TP VS TN	167.	2713.60	27.675	168.	2741.30	27.791
TP VS TN	169.	2769.10	27.907	170.	2797.10	28.022
TP VS TN	171.	2825.20	28.137	172.	2853.40	28.252
TP VS TN	173.	2881.70	28.366	174.	2910.10	28.480
TP VS TN	175.	2938.60	28.594	176.	2967.30	28.708
TP VS TN	177.	2996.10	28.822	178.	3025.00	28.935
TP VS TN	179.	3054.00	29.048	180.	3083.10	29.161
TP VS TN	181.	3112.30	29.274	182.	3141.60	29.387
TP VS TN	183.	3171.00	29.499	184.	3200.60	29.611
TP VS TN	185.	3230.30	29.723	186.	3260.10	29.835
TP VS TN	187.	3290.00	29.946	188.	3320.00	30.057
TP VS TN	189.	3350.10	30.168	190.	3380.30	30.279
TP VS TN	191.	3410.60	30.389	192.	3441.00	30.499
TP VS TN	193.	3471.60	30.609	194.	3502.30	30.719
TP VS TN	195.	3533.10	30.829	196.	3564.00	30.938
TP VS TN	197.	3595.00	31.047	198.	3626.10	31.156
TP VS TN	199.	3657.30	31.265	200.	3688.60	31.373
TP VS TN	201.	3720.00	31.481	202.	3751.50	31.589
TP VS TN	203.	3783.10	31.697	204.	3814.90	31.805
TP VS TN	205.	3846.80	31.912	206.	3878.80	32.019
TP VS TN	207.	3910.80	32.126	208.	3943.00	32.233
TP VS TN	209.	3975.30	32.339	210.	4007.70	32.445

TP VS TN	211.	4040.20	32.551	212.	4072.80	32.657
TP VS TN	213.	4105.50	32.763	214.	4138.30	32.868
TP VS TN	215.	4171.20	32.973	216.	4204.30	33.078
TP VS TN	217.	4237.40	33.183	218.	4270.60	33.287
TP VS TN	219.	4303.90	33.391	220.	4337.30	33.495
TP VS TN	221.	4370.80	33.599	222.	4404.40	33.703
TP VS TN	223.	4438.20	33.806	224.	4472.10	33.909
TP VS TN	225.	4506.10	34.012	226.	4540.20	34.115
TP VS TN	227.	4574.40	34.217	228.	4608.70	34.319
TP VS TN	229.	4643.00	34.421	230.	4677.50	34.523
TP VS TN	231.	4712.10	34.624	232.	4746.80	34.725
TP VS TN	233.	4781.50	34.826	234.	4816.40	34.927
TP VS TN	235.	4851.40	35.028	236.	4886.50	35.128
TP VS TN	237.	4921.60	35.228	238.	4956.90	35.328
TP VS TN	239.	4992.30	35.428	240.	5027.80	35.528
TP VS TN	241.	5063.40	35.627	242.	5099.00	35.726
TP VS TN	243.	5134.80	35.825	244.	5170.70	35.923
TP VS TN	245.	5206.70	36.021	246.	5242.70	36.119
TP VS TN	247.	5278.90	36.217	248.	5315.20	36.315
TP VS TN	249.	5351.60	36.413	250.	5388.10	36.510
TP VS TN	251.	5424.70	36.607	252.	5461.40	36.704
TP VS TN	253.	5498.20	36.800	254.	5535.00	36.896
TP VS TN	255.	5571.90	36.992	256.	5608.90	37.088
TP VS TN	257.	5646.00	37.184	258.	5683.20	37.280
TP VS TN	259.	5720.50	37.375	260.	5757.90	37.470
TP VS TN	261.	5795.40	37.565	262.	5833.00	37.659
TP VS TN	263.	5870.70	37.753	264.	5908.50	37.847
TP VS TN	265.	5946.40	37.941	266.	5984.40	38.035
TP VS TN	267.	6022.50	38.129	268.	6060.70	38.222

TP VS TN	269.	6099.00	38.315	270.	6137.40	38.408
TP VS TN	271.	6175.90	38.500	272.	6214.40	38.592
TP VS TN	273.	6253.00	38.684	274.	6291.70	38.776
TP VS TN	275.	6330.50	38.868	276.	6369.40	38.959
TP VS TN	277.	6408.40	39.050	278.	6447.50	39.141
TP VS TN	279.	6486.70	39.232	280.	6526.00	39.323
TP VS TN	281.	6565.40	39.413	282.	6604.90	39.503
TP VS TN	283.	6644.40	39.593	284.	6684.00	39.682
TP VS TN	285.	6723.70	39.771	286.	6763.50	39.860
TP VS TN	287.	6803.40	39.949	288.	6843.40	40.038
TP VS TN	289.	6883.50	40.127	290.	6923.70	40.215
TP VS TN	291.	6964.00	40.303	292.	7004.30	40.391
TP VS TN	293.	7044.70	40.479	294.	7085.20	40.566
TP VS TN	295.	7125.80	40.653	296.	7166.50	40.740
TP VS TN	297.	7207.30	40.827	298.	7248.20	40.913
TP VS TN	299.	7289.20	40.999	300.	7330.20	41.085

INPUT DATA CARDS (SAMPLE)

```
DEG. K        90.27   77.42     220.      77.347          NO
LN2-LOX CALIB         NO 1     M.D.MAYNARD          15 APRIL 1966
REPEAT LAST T.C. DECK                                0    DEG. K        YES
```

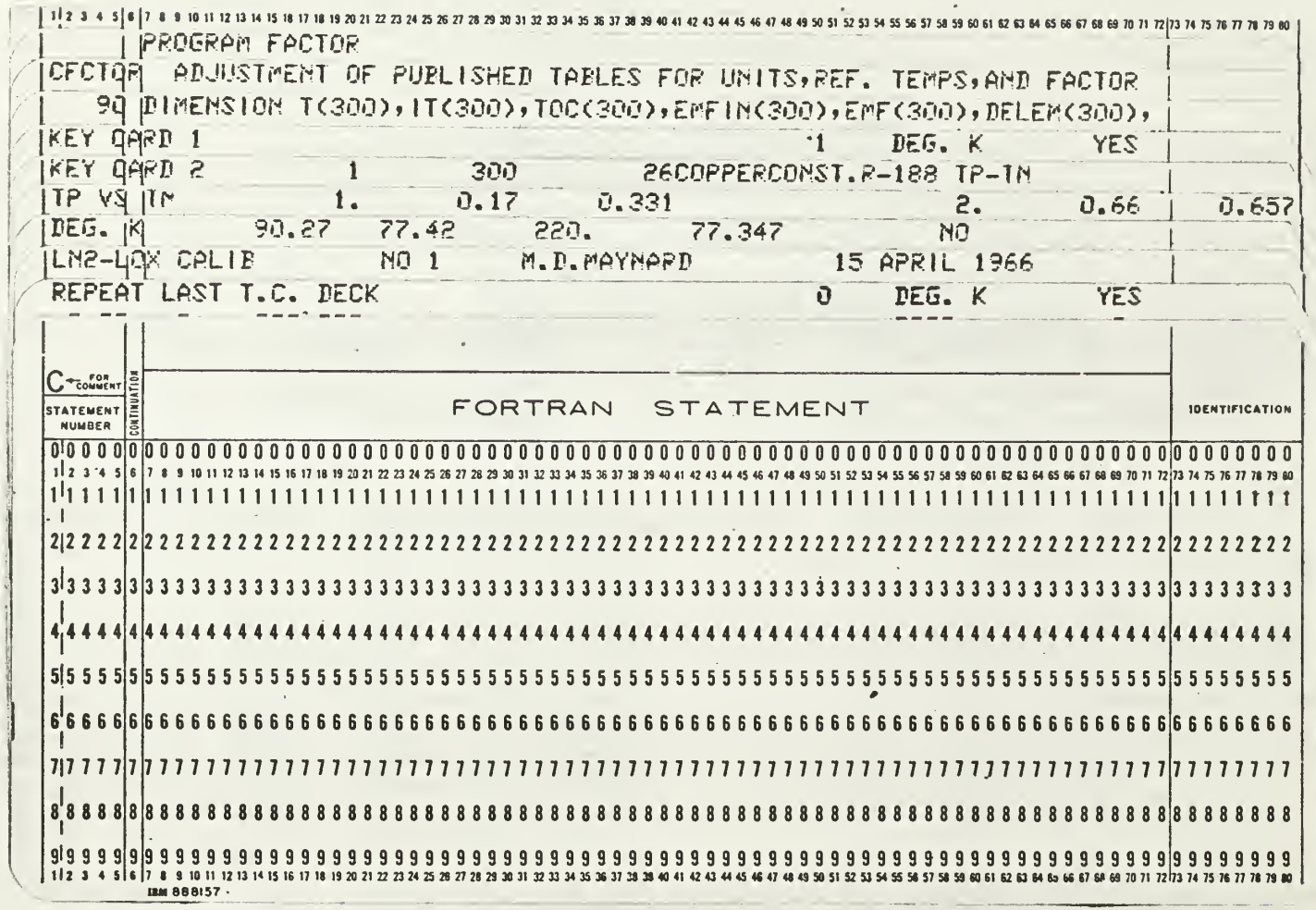

SAMPLE CARDS FOR COLUMN SPACING

TABLE B-I

SAMPLE OF GENERATED WORKING TABLE

THERMOCOUPLE TABLE FOR COPPER VS CONST., ISA TYPE TP-TN , BASED ON NAT. BUR. OF STANDARDS PUB. R-188 WITH CALC. MULT. FACTOR OF .99451. LN2-LOX CALIB , LOT NO 1 . USERS REFERENCE TEMPERATURE 77.347 DEG. K
TEST DATE 15 APRIL 1966 BY M.D.MAYNARD

TEMP DEG K	EMF MIC V	DELEMF MIC V	DE/DT MIC V/DGK	TEMP DEG K	EMF MIC V	DELEMF MIC V	DE/DT MIC V/DGK
81	60.2	16.6	16.754	121	834.6	21.9	21.906
82	77.0	16.8	16.886	122	856.6	22.0	22.031
83	93.9	16.9	17.018	123	878.7	22.1	22.157
84	111.0	17.1	17.150	124	900.9	22.2	22.282
85	128.2	17.2	17.283	125	923.2	22.3	22.406
86	145.5	17.3	17.415	126	945.7	22.5	22.531
87	163.0	17.5	17.547	127	968.3	22.6	22.655
88	180.6	17.6	17.679	128	991.0	22.7	22.779
89	198.4	17.8	17.812	129	1013.8	22.8	22.904
90	216.3	17.9	17.944	130	1036.8	23.0	23.028
91	234.3	18.0	18.076	131	1059.9	23.1	23.153
92	252.4	18.1	18.209	132	1083.1	23.2	23.279
93	270.7	18.3	18.340	133	1106.5	23.4	23.404
94	289.1	18.4	18.471	134	1130.0	23.5	23.529
95	307.6	18.5	18.602	135	1153.6	23.6	23.654
96	326.3	18.7	18.733	136	1177.2	23.6	23.779
97	345.1	18.8	18.863	137	1201.1	23.9	23.904
98	364.0	18.9	18.992	138	1225.1	24.0	24.029
99	383.1	19.1	19.122	139	1249.1	24.0	24.155
100	402.3	19.2	19.251	140	1273.3	24.2	24.280

APPENDIX C

Sample Calculation with Error Analysis

The following are assumptions used in reducing data:

a. Temperature tables in microvolts are accurate to within $\pm 1\ \mu V$ (see Appendix A) from 77.3 K to 90.1°K and within $\pm 2\ \mu V$ above 90.1°K.

b. Liquid nitrogen used had a minimum purity of 99.95% and the same quality used for calibration.

c. Thermocouple hot junction positions are known to $\pm$ .01 inches.

d. Thermal conductivities of electrical tough pitch copper agree with tabulated values within 5%.

e. Barometric pressure was accurate to $\pm$ 0.1 mm Hg.

f. Measured depths of nitrogen are to within 1 cm. The reference thermocouple was always in 10 cm of nitrogen.

Arbitrarily choosing point 8 of the oxidized copper surface with a barometric pressure of 766.8 mm Hg at 21.2°C.

TABLE C-1

ZERO CORRECTED AND REDUCED THERMOCOUPLE DATA

T. C.	Location from Boiling Surface (inches)	E. M. F. μV	Corrected Temperature for Barom. and Reference Immer. Depth °K
1	.060 $\pm$ .010	116. $\pm$ 2.	84.42 $\pm$ .12
2	.300 $\pm$ .010	142. $\pm$ 2.	85.90 $\pm$ .12
3	.530 $\pm$ .010	167. $\pm$ 2.	87.30 $\pm$ .11
4	.763 $\pm$ .010	195. $\pm$ 2.	88.90 $\pm$ .11

The saturation temperature correction for barometer and reference immersion depth was similar to the calculation of the saturation temperature correction used for working fluid shown below.

T Saturation

Depth of LN_2 at beginning of run was 42 cm and at the end was 32 cm, therefore, for error purposes, the average was assumed to be 37 ± 5 cm.

Using the standard pressure depth equation and changing units:

$$P_{head} = \gamma H = \left(\frac{50.4 lb}{ft^3}\right)\left(\frac{37 \pm 5 cm}{2.54 cm/in}\right)\left(\frac{ft^3}{1728 in^3}\right)\left(\frac{760 mm}{14.7 lb/in^2}\right) \qquad (C\text{-}1)$$

$$P_{head} = 21.96 \pm 2.97 \text{ mm Hg}$$

$$\Delta P_b = P_b - P_o = 760.0 - 766.80 \pm .1 \qquad (C\text{-}2)$$

$$\Delta P_b = 6.80 \pm .1 \text{ mm Hg}$$

P_c was taken by four way interpolation from Ref. [11] for barometric pressure and temperature.

$$P_c = -2.3 \text{mm Hg}$$

$$\Delta P_{total} = P_{head} + \Delta P_b + P_c \qquad (C\text{-}3)$$

$$= 21.96 + 6.8 - 2.3$$

$$\Delta P_{total} = 26.46 \pm 2.97$$

Making use of the perfect gas relationship, the Clausius-Clapeyron equation takes the form:

$$\Delta T_s = \frac{R T_o^2}{h_{fg}} \frac{\Delta P_{total}}{P_o} \qquad (C\text{-}4)$$

$$= \left(\frac{.07088 btu}{lb}\right)\left(\frac{lb}{85.7 btu}\right)\ \frac{(139 °R)^2}{}\ \left(\frac{\Delta P_{total} \text{ mm hg}}{760. \text{ mm hg}}\right)\left(\frac{5°K}{9°R}\right)$$

$$= .1167\, \Delta P_{total}\ °K$$

Substituting from above:

$$\Delta T_s = (.1167)\ (26.46 \pm 2.97)$$

$$\Delta T_s = .309 \pm .035 \text{ K}$$

$$T_s = T_o \text{ (tabulated [27])} + \Delta T_s \qquad (C\text{-}5)$$

$$= 77.347 + (.309 \pm .035)$$

$$= 77.66 \pm .04 °K$$

Heat Flux

By plotting T. C. temperature readings versus position from the boiling surface with error limits included, and connecting the extreme points of the data, minimum and maximum sloped lines ($\partial T/\partial X$) for these points can be determined.

Using the Fourier conduction equation and knowing the thermal conductivity k_w based on average temperature (°K) between T. C. position 1 and 4 (Figure 10),

$$Q/A = \frac{k_w \partial T}{\partial X} \approx \frac{k_w \Delta T}{\Delta X} = \left(\frac{4.91 W}{cm\,°K}\right)\left(\frac{4.48°K}{.703 in}\right)\left(\frac{in.}{2.54 cm}\right) \qquad (C\text{-}6)$$

For the sample data listed, Q/A maximum = 12.42 watts/cm^2 and Q/A minimum = 11.20 watts/cm^2 for an average of Q/A = 12.31 $\pm$ 1.11 watts/cm^2.

T Wall

Altering equation (C-6) gives:

$$T_1 - T_w = Q/A \frac{X_1}{k_1} \qquad (C\text{-}7)$$

where subscript 1 indicates thermocouple 1 position.

Substitution of the average Q/A into (C-7) gives:

$$T_1 - T_w = \left(\frac{12.31 W}{cm^2}\right)(.06 \text{ inches})\left(\frac{2.54 cm}{(in)}\right)\left(\frac{cm\,°K}{(5.03W)}\right)$$

$$T_1 - T_w = .373°K$$

Using the value of T_1 = 84.42 from table B-1

$$T_w = 84.42 - .373 = 84.05\ °K$$

The most probable error for the wall temperature is:

$$\Delta T_w = \sqrt{\left(\Delta T_1\right)^2 + (T_1 - T_w)^2\left[\left(\frac{\Delta Q/A}{Q/A}\right)^2 + \left(\frac{\Delta k}{k}\right)^2 + \left(\frac{\Delta X_1}{X_1}\right)^2\right]} \qquad (C\text{-}8)$$

$\frac{\Delta Q/A}{Q/A}$ = fractional error in heat flux = .0891

$\frac{\Delta k_w}{k_w}$ = fractional error in thermal conductivity = .050

$\frac{\Delta x_1}{x_1}$ = fractional error in thermocouple 1 position = .166

ΔT_1 = ± .12° from the temperature reduction (Table B-1)

Substituting in equation (C-8)

ΔT_w = ± .14°K

$T_{wall} - T_{saturation}$

Simple subtraction gives the following for a value of

$\Delta T = T_w - T_s = (84.05 \pm 0.14) - (77.66 \pm 0.04) = 6.39 \pm .15$°K

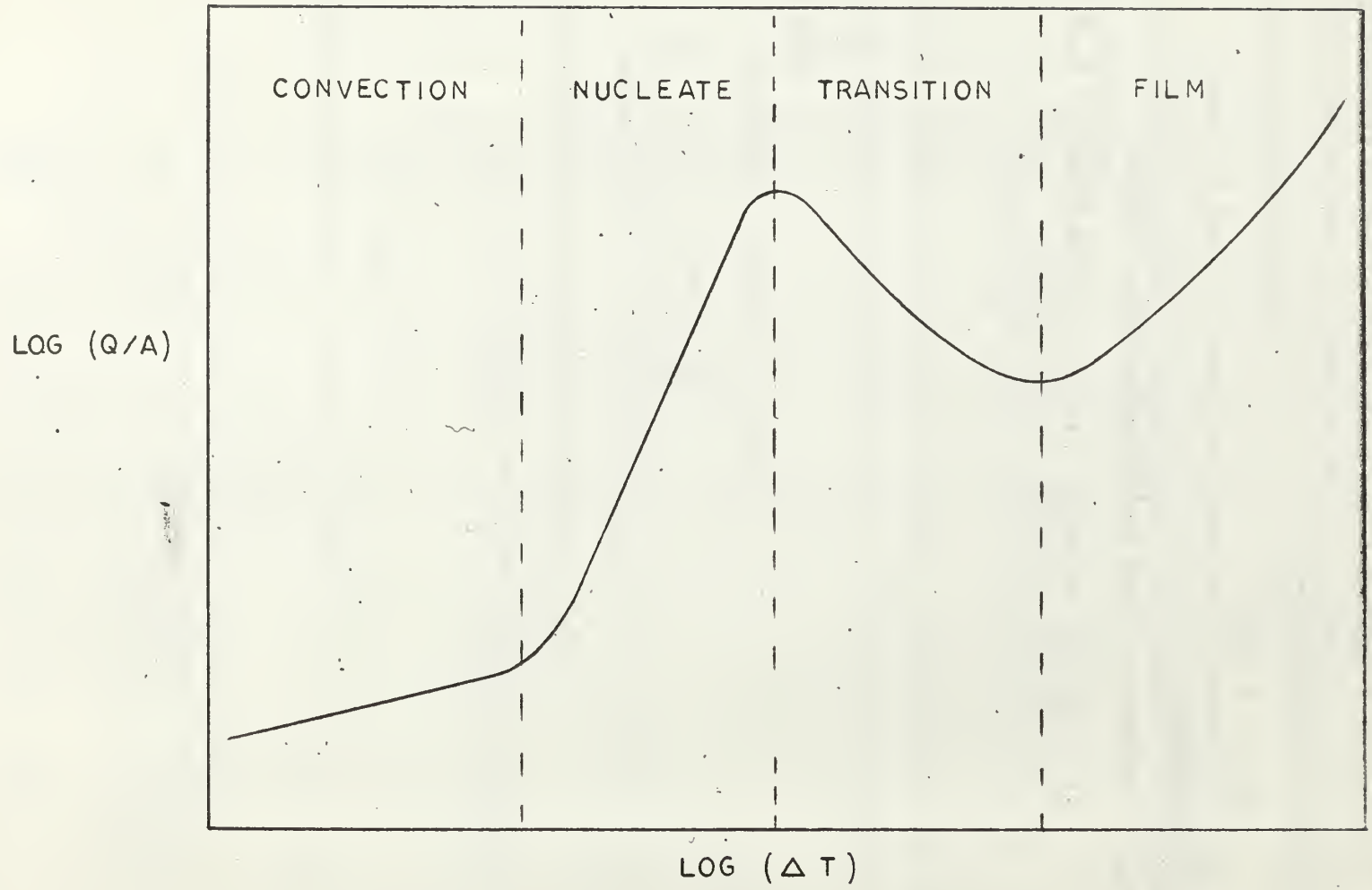

FIG. 1 TYPICAL BOILING CURVE

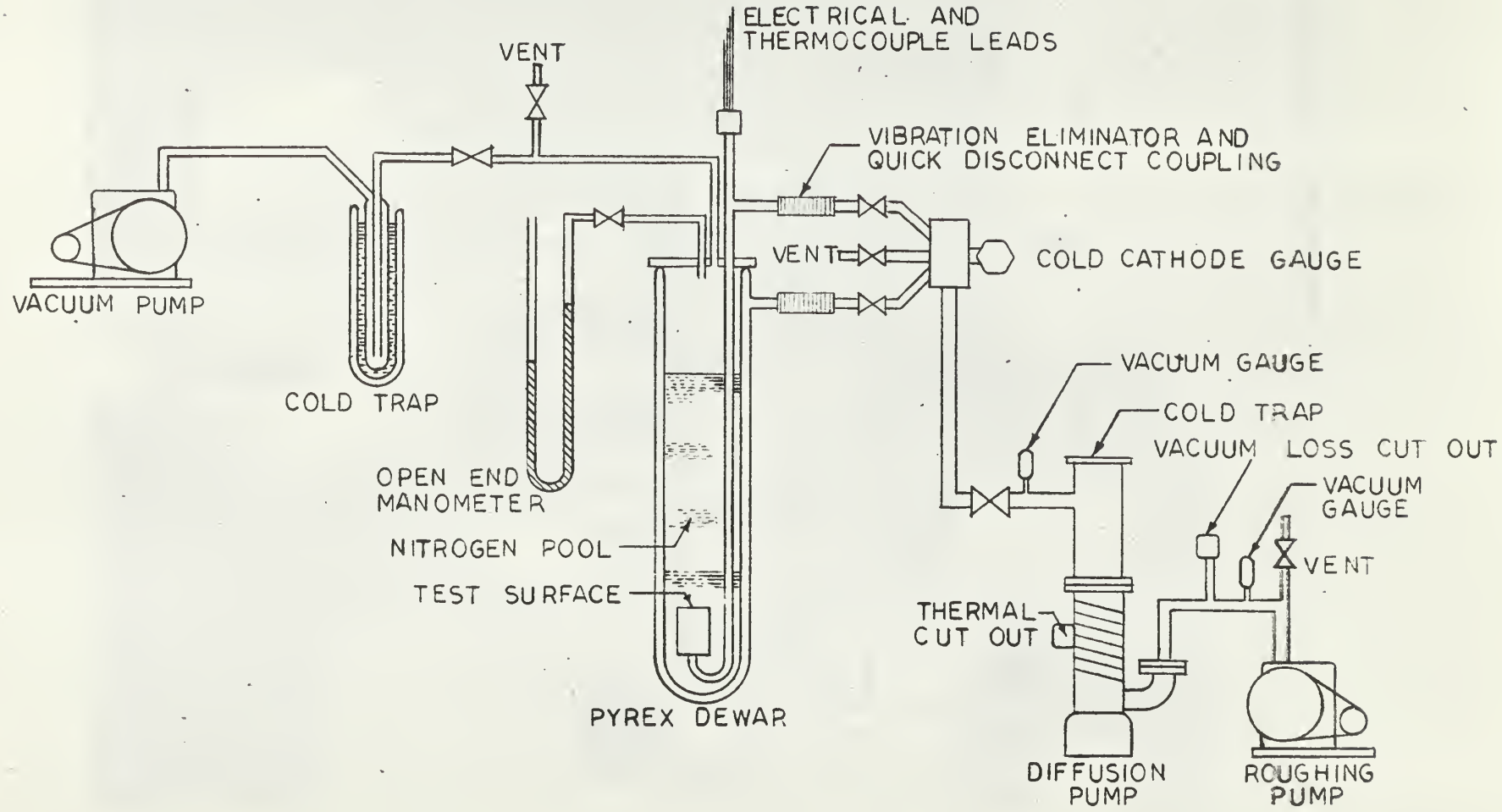

FIG. 2 SCHEMATIC DIAGRAM OF APPARATUS

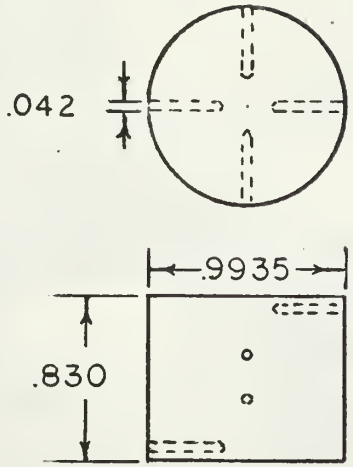

ELECTRICAL
TOUGH PITCH
COPPER

T.C.	℄ DISTANCE TO BOILER SURFACE
1.	.060 IN.
2.	.300 IN.
3.	.530 IN.
4.	.763 IN.

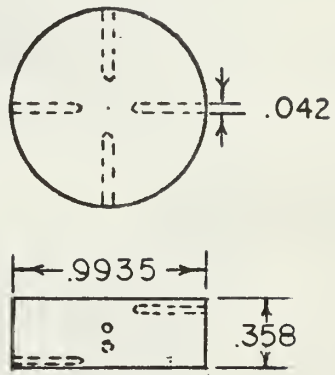

NICKEL 200

T.C.	℄ DISTANCE TO BOILER SURFACE
1.	.073 IN.
2.	.156 IN.
3.	.232 IN.
4.	.307 IN.

FIG. 5 DETAILS OF BOILERS

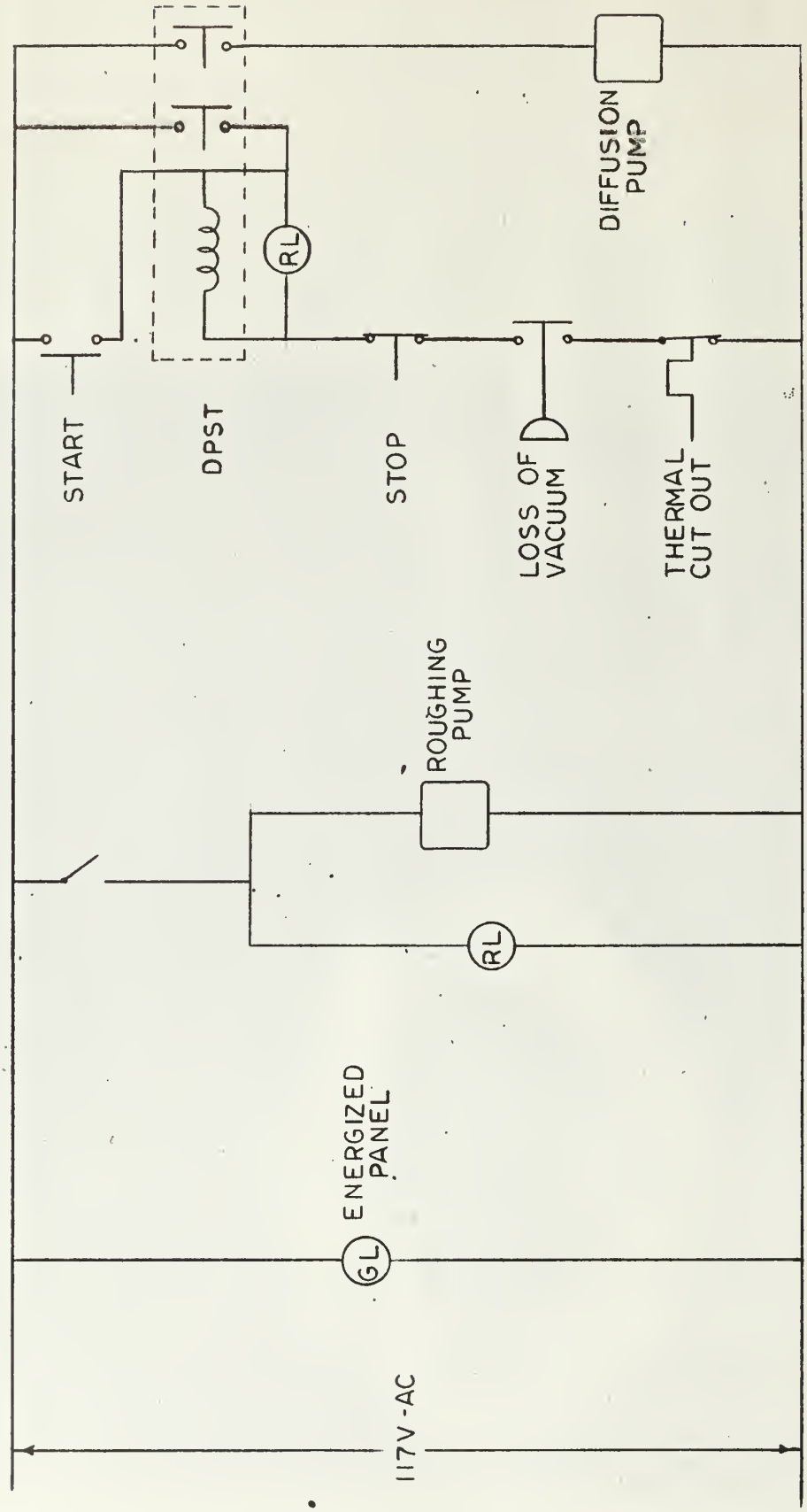

FIG.7 ELECTRICAL DIAGRAM FOR VACUUM SYSTEM CONTROL

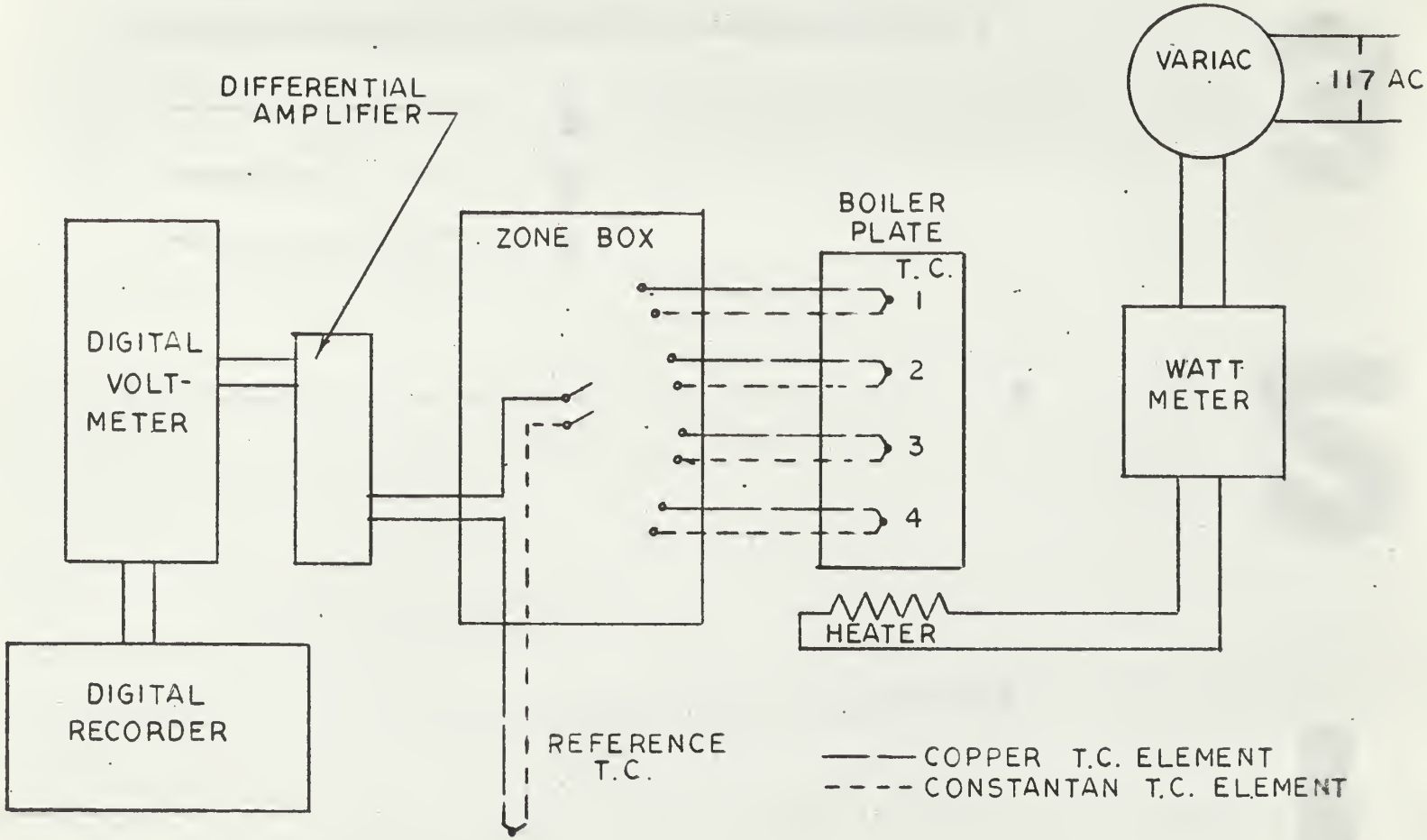

FIG. 8 SCHEMATIC DIAGRAM OF HEATER CONTROL AND TEMPERATURE MEASUREMENT CIRCUITS

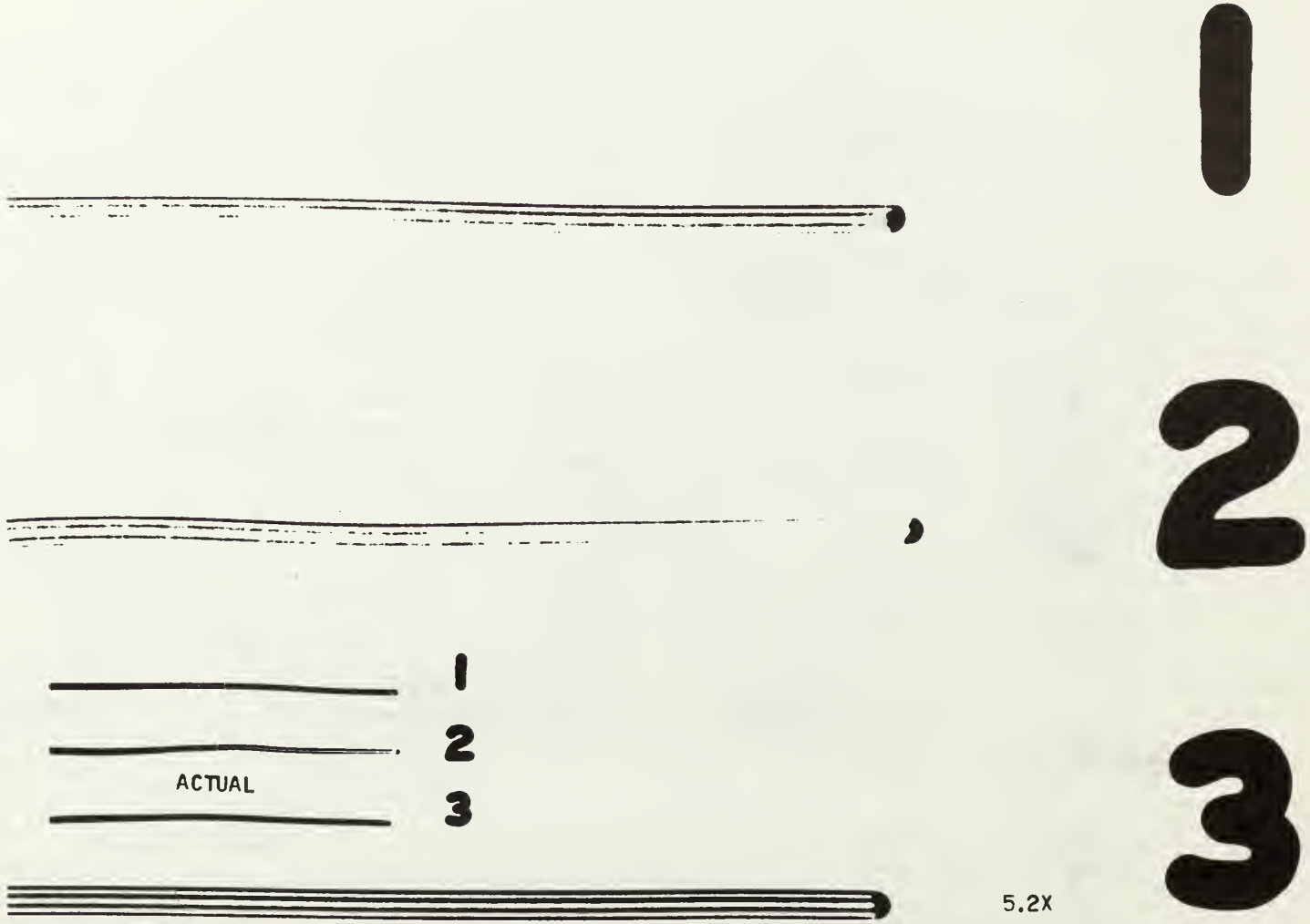

FIG. 9 THERMOCOUPLE X-RAY VIEW WITH MAGNIFICATION OF HOT JUNCTION

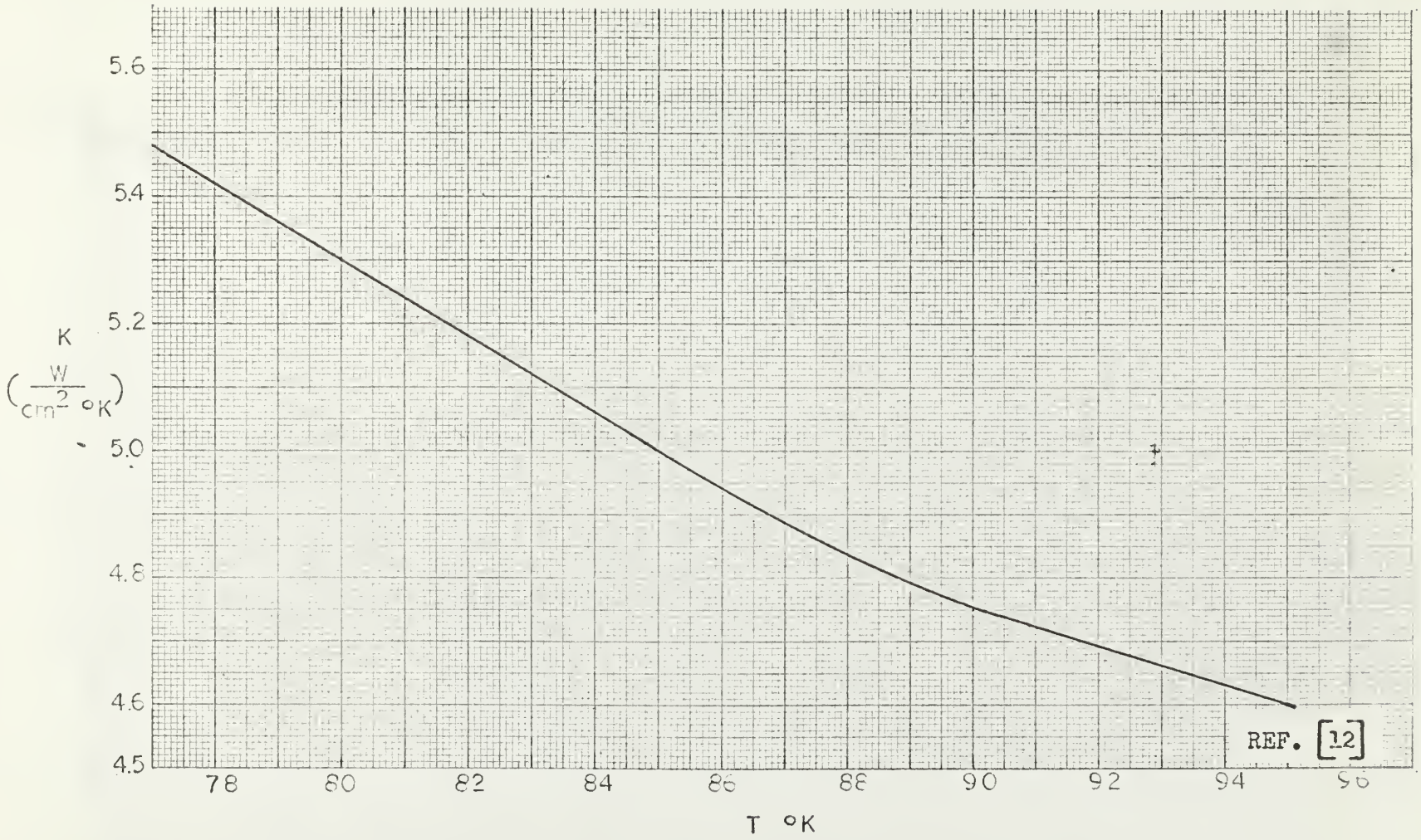

FIG. 10 THERMAL CONDUCTIVITY OF COPPER USED IN TEST ELEMENT

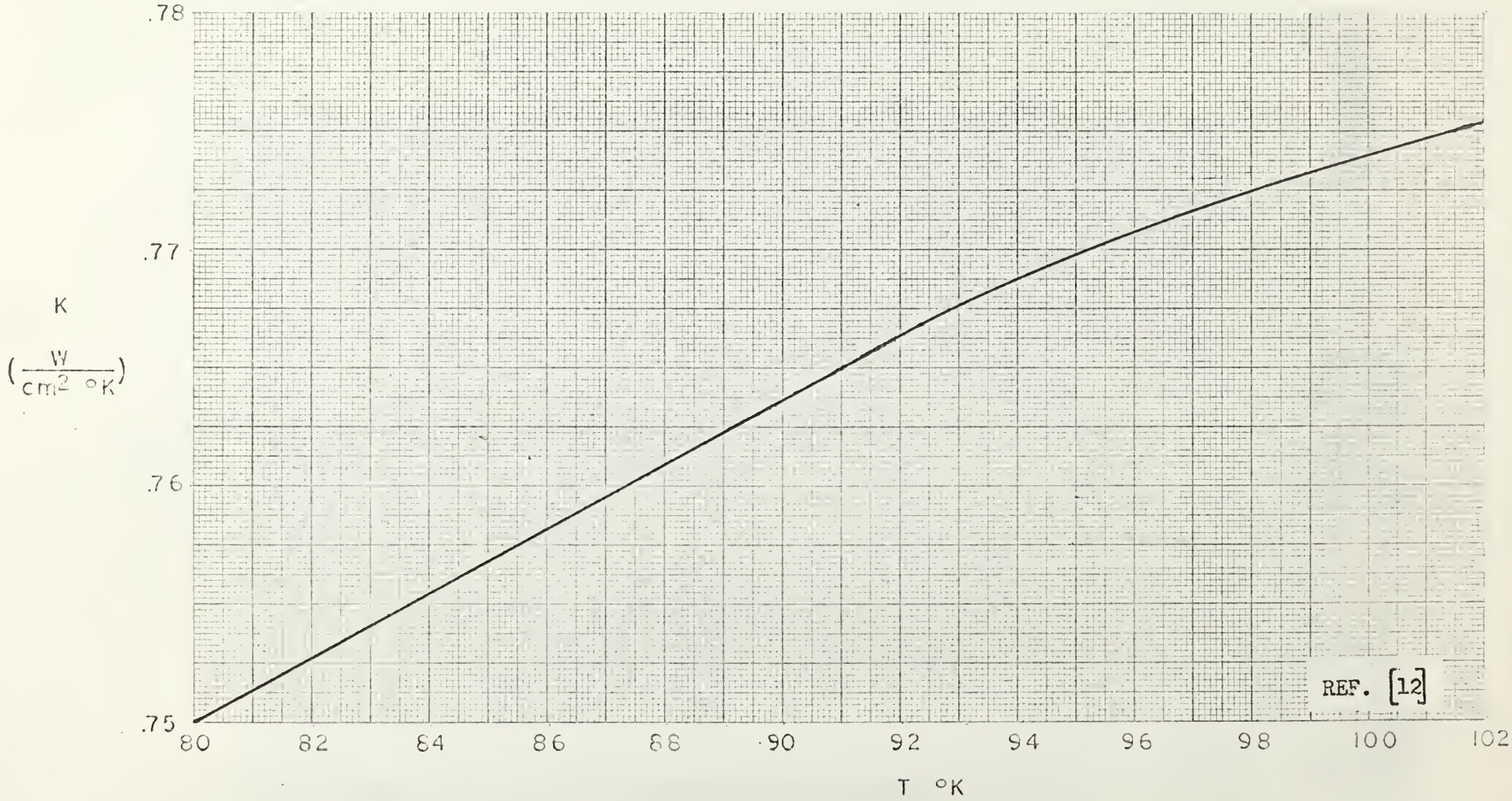

FIG. II THERMAL CONDUCTIVITY OF NICKEL 200 USED IN TEST ELEMENT

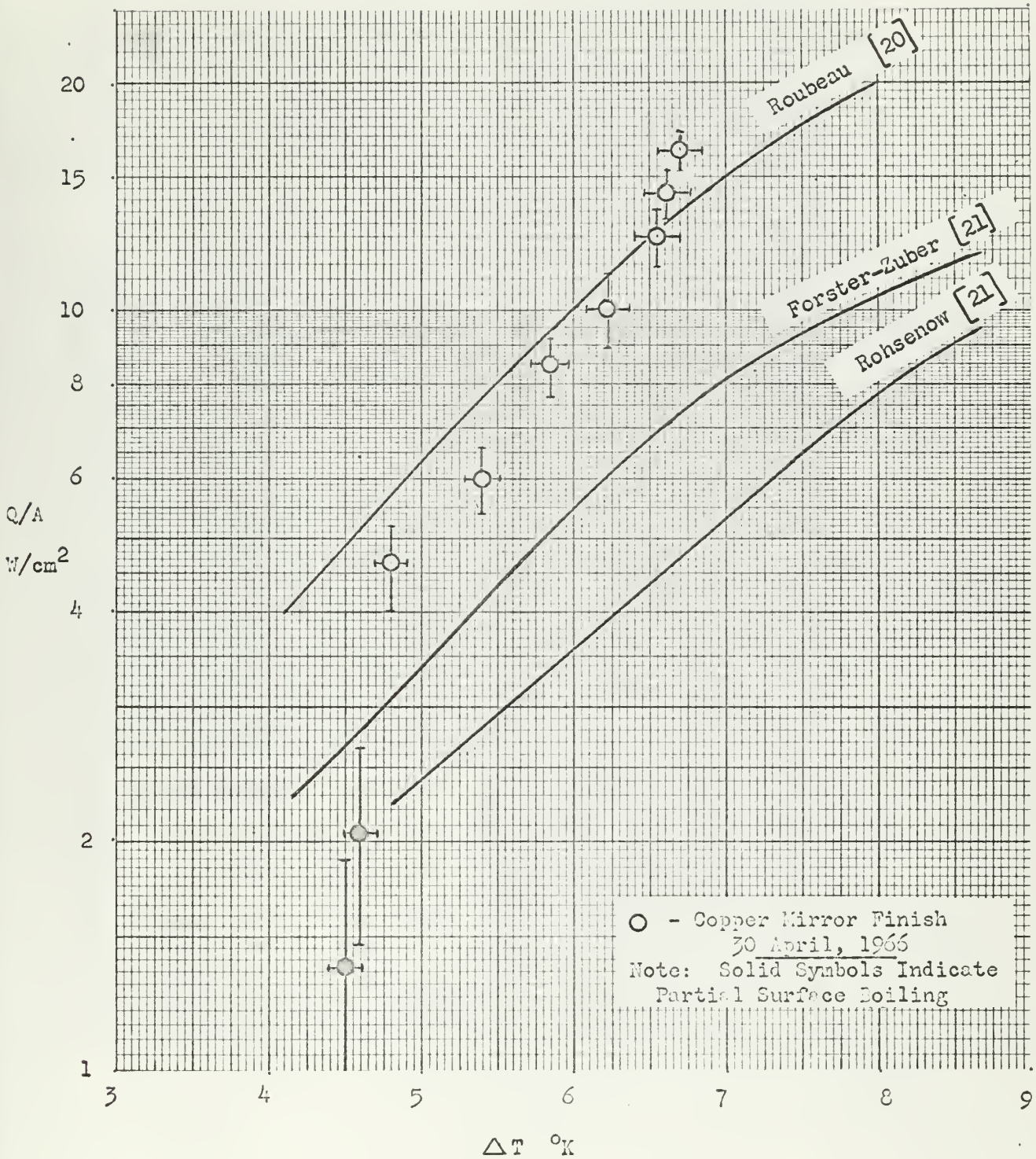

FIG. 12 SAMPLE DATA WITH EXPERIMENTAL ERROR LIMITS SHOWING DATA OF ROUBEAU AND THEORETICAL CORRELATIONS OF ROHSENOW AND FORSTER-ZUBER

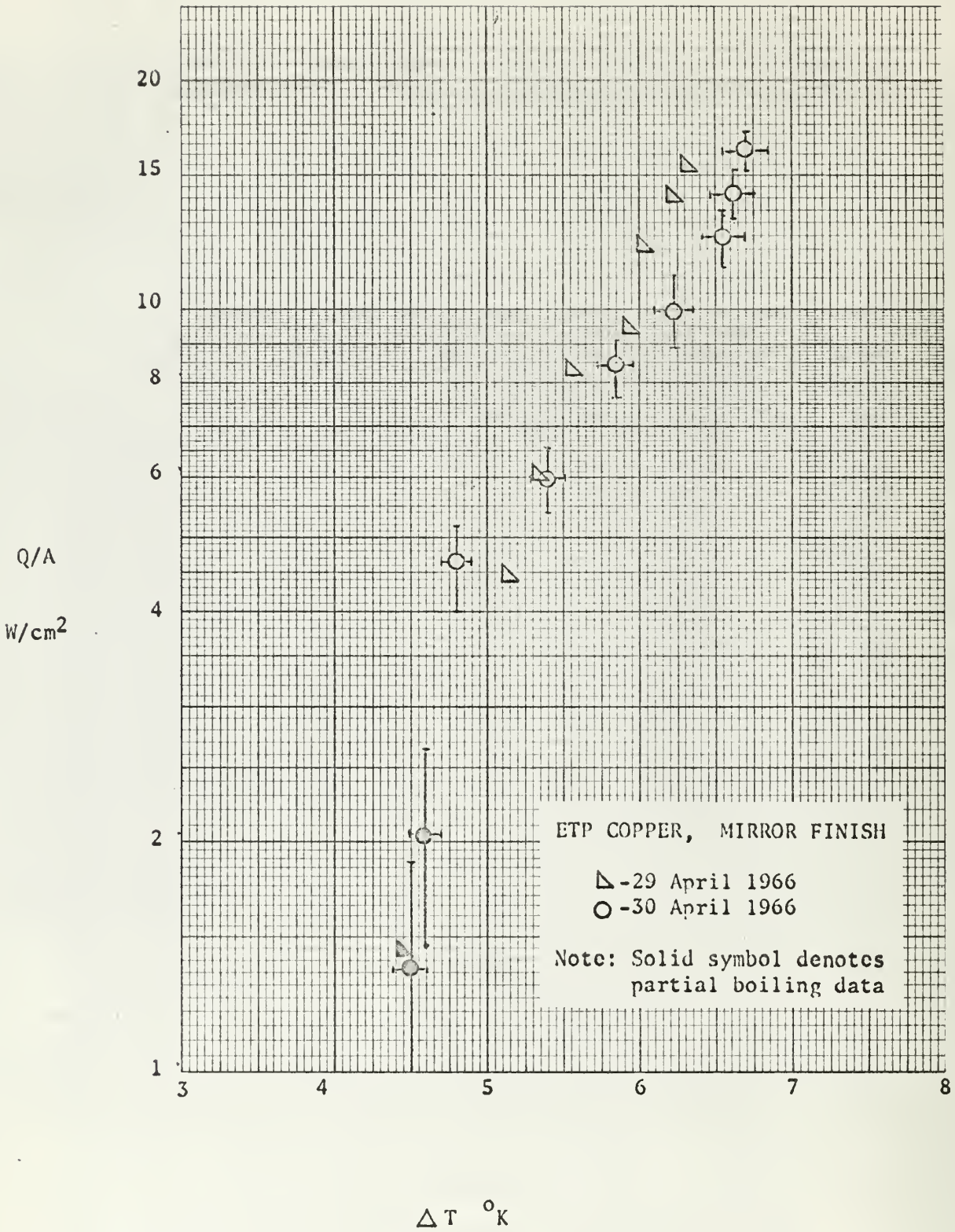

FIG. 13 REPRODUCIBILITY OF NUCLEATE BOILING RESULTS

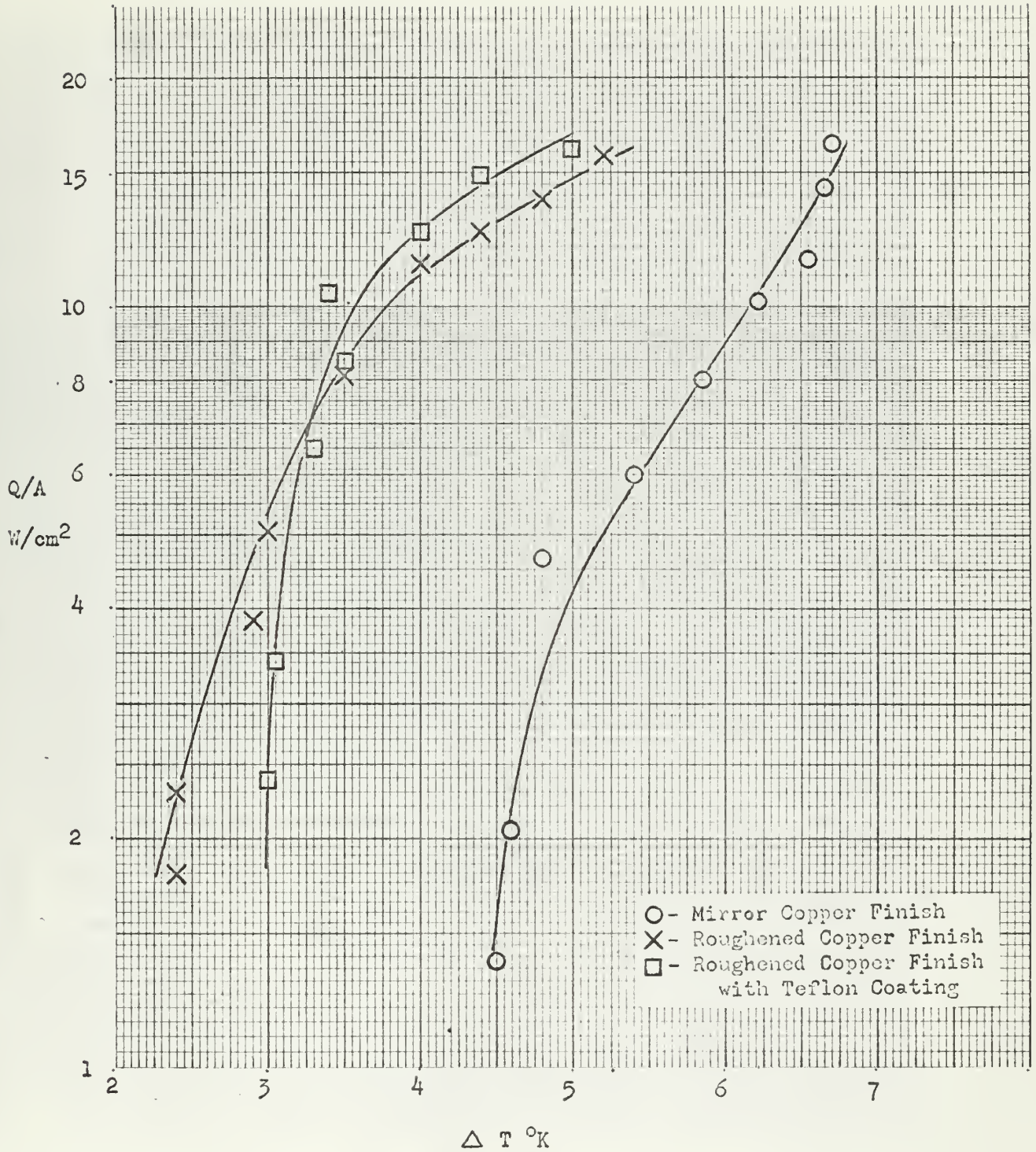

FIG. 14 EFFECT OF SURFACE ROUGHNESS ON NUCLEATE POOL BOILING OF LIQUID NITROGEN

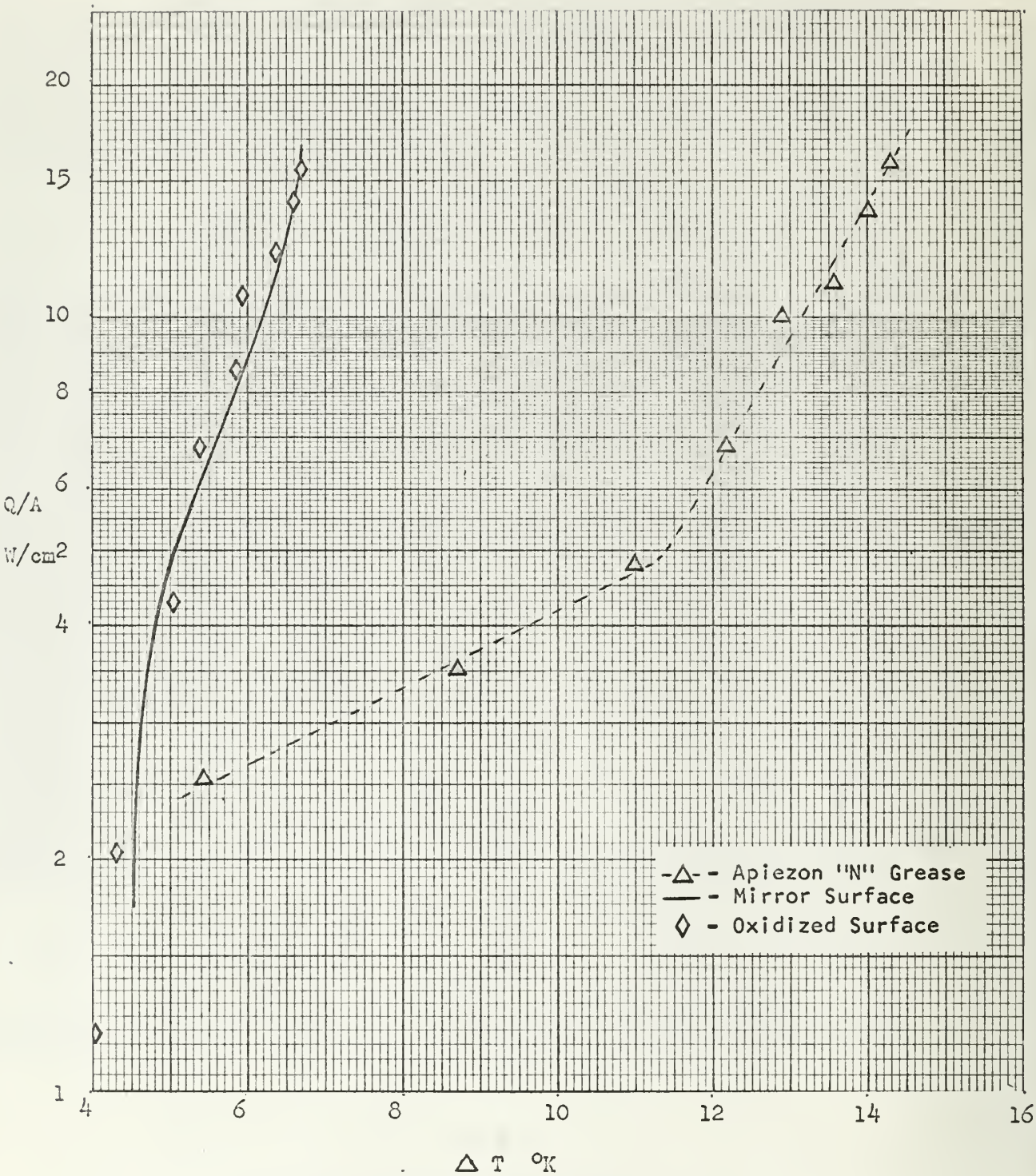

FIG. 15 EFFECT OF SURFACE CONTAMINANTS ON NUCLEATE POOL BOILING OF LIQUID NITROGEN

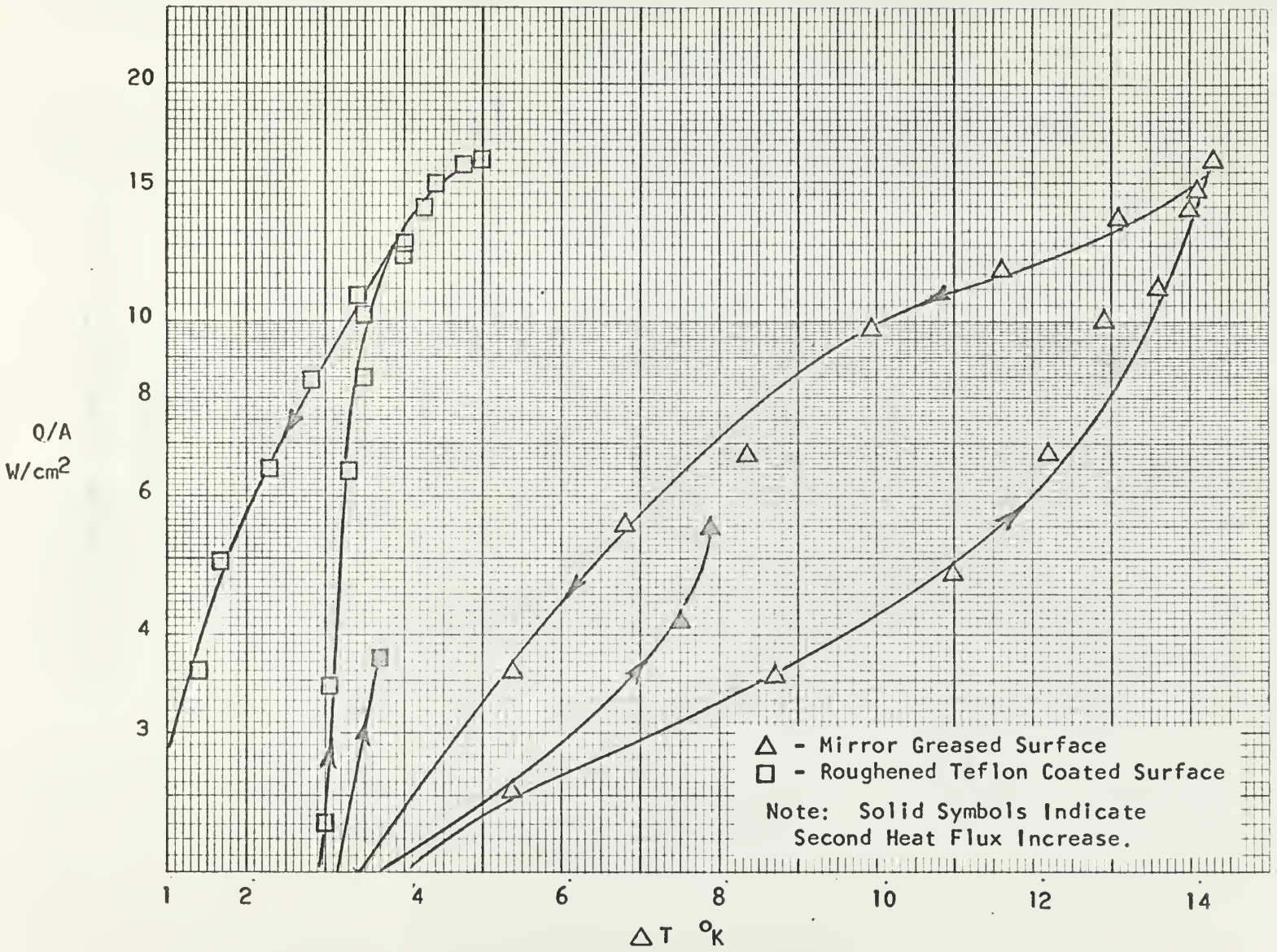

FIG. 16 HYSTERESIS EFFECTS WITH TEFLON AND APIEZON "N" GREASE ON COPPER SURFACE

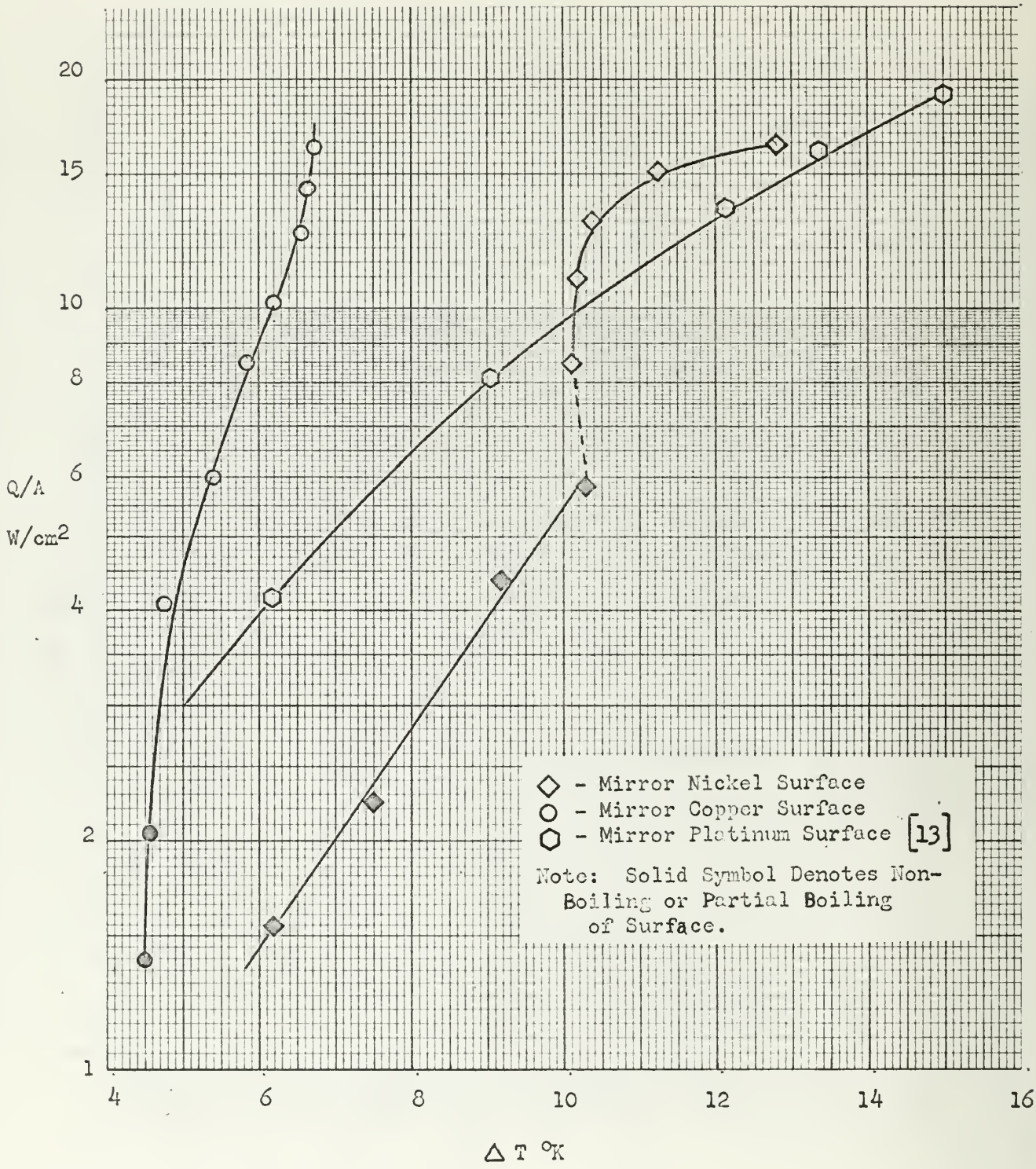

FIG. 17 EFFECT OF BOILER MATERIALS

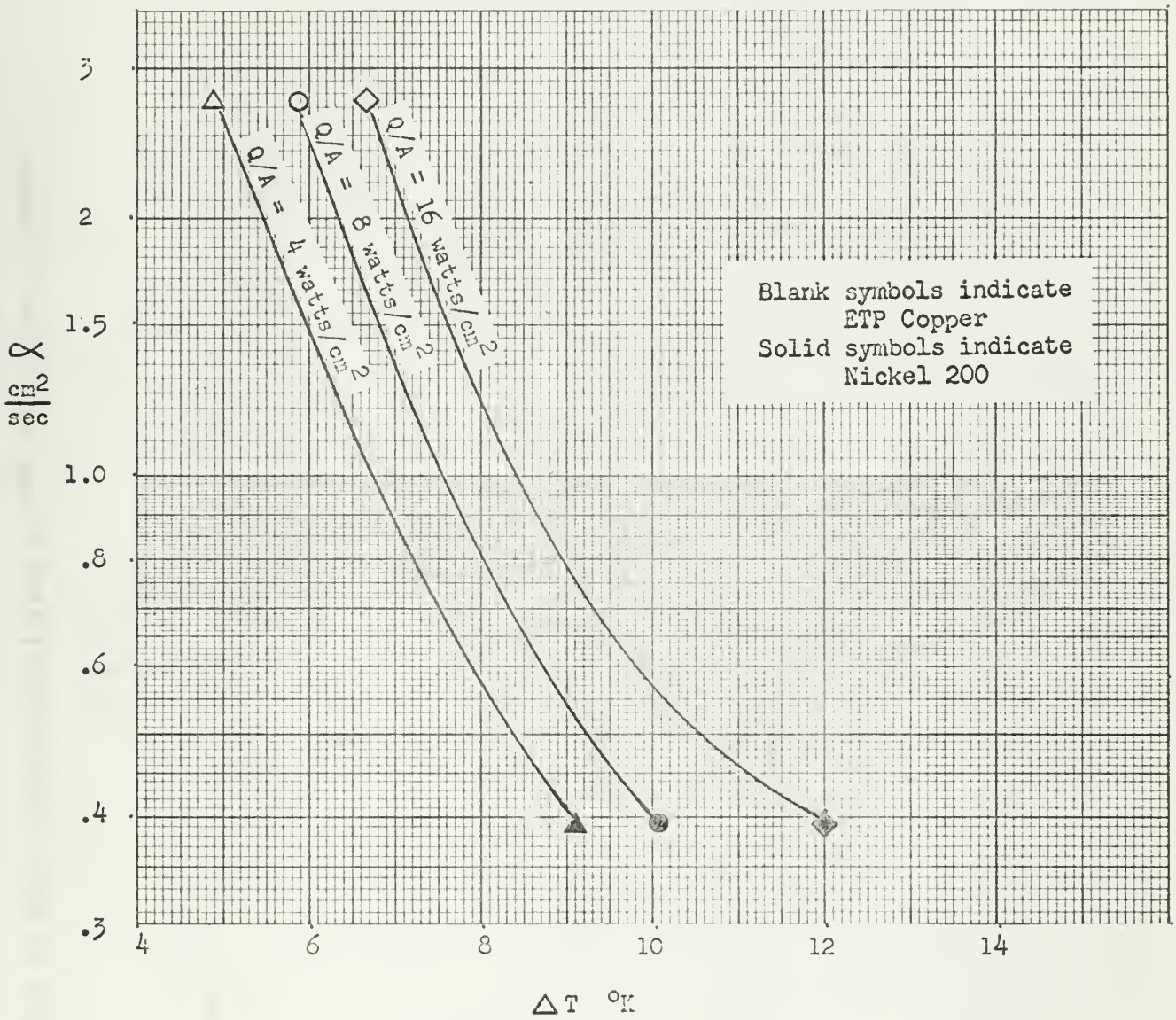

FIG. 18 EFFECT OF MATERIAL THERMAL DIFFUSIVITY ON NUCLEATE BOILING WALL SUPERHEAT ($T_w - T_s$)

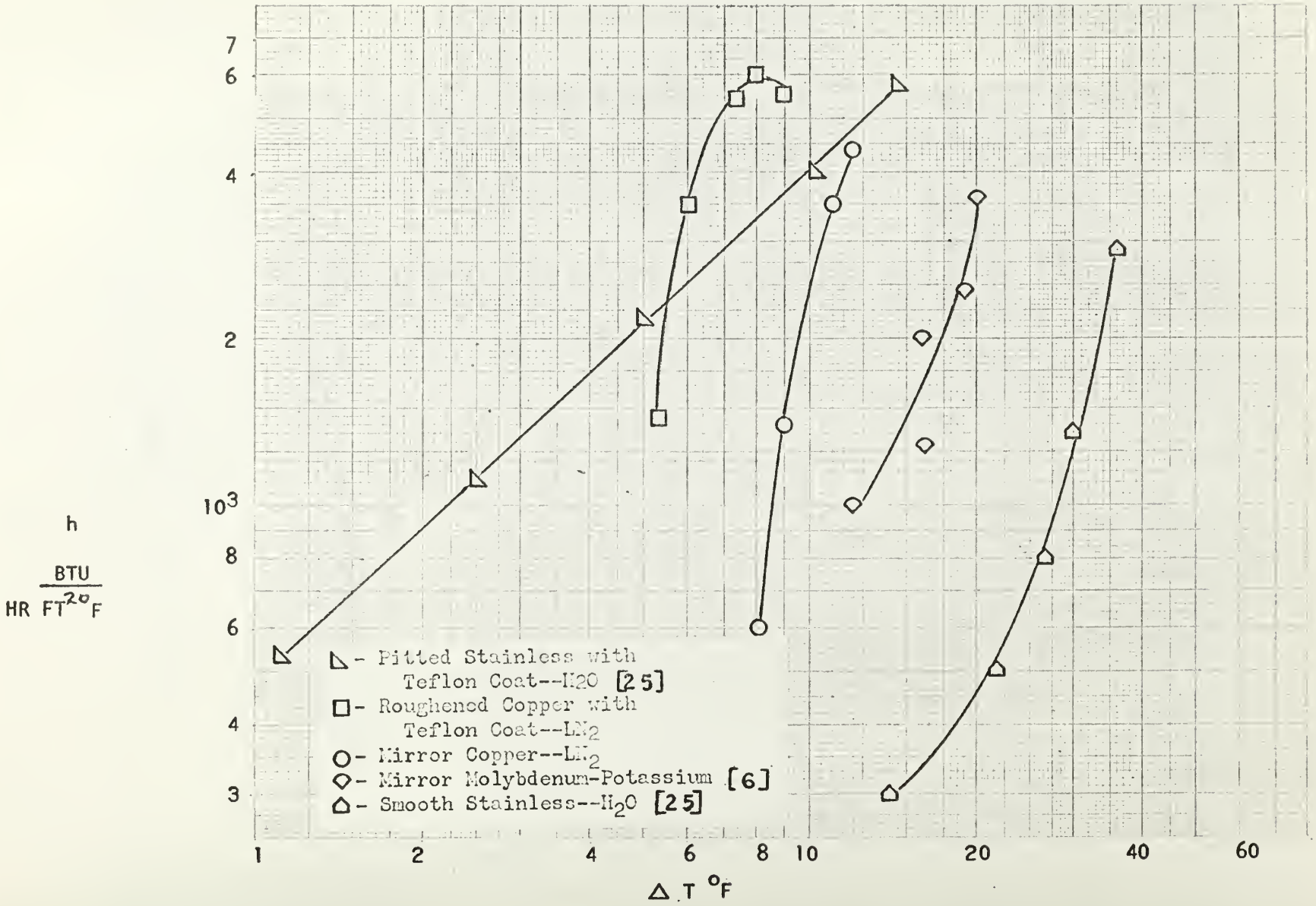

FIG. 19 COMPARISON OF HEAT TRANSFER COEFFICIENT OF LN_2, WATER, AND POTASSIUM

INITIAL DISTRIBUTION LIST

		No. Copies
1.	Defense Documentation Center Cameron Station Alexandria, Virginia 22314	20
2.	Library U.S. Naval Postgraduate School Monterey, California 93940	2
3.	LT P. J. Marto, USNR (Thesis Advisor) Department of Mechanical Engineering U.S. Naval Postgraduate School Monterey, California 93940	12
4.	Professor D. N. Lyon Chairman, Department of Chemistry University of California Berkeley, California	1
5.	LT M. D. Maynard, USN U.S.S. LEXINGTON (CVS-16) % Fleet Post Office New York, N.Y.	1

Security Classification

DOCUMENT CONTROL DATA - R&D

(Security classification of title, body of abstract and indexing annotation must be entered when the overall report is classified)

1. ORIGINATING ACTIVITY (Corporate author)	2a. REPORT SECURITY CLASSIFICATION
U.S. Naval Postgraduate School Monterey, California	UNCLASSIFIED
	2b. GROUP

3. REPORT TITLE

AN EXPERIMENTAL INVESTIGATION OF THE EFFECT OF SURFACE CONDITIONS ON NUCLEATE POOL BOILING HEAT TRANSFER TO LIQUID NITROGEN FROM A HORIZONTAL SURFACE

4. DESCRIPTIVE NOTES (Type of report and inclusive dates)

Thesis

5. AUTHOR(S) (Last name, first name, initial)

MAYNARD, Michael D., LT, USN, 630733

6. REPORT DATE	7a. TOTAL NO. OF PAGES	7b. NO. OF REFS
May 1966	82	28

8a. CONTRACT OR GRANT NO.	9a. ORIGINATOR'S REPORT NUMBER(S)
b. PROJECT NO.	
c.	9b. OTHER REPORT NO(S) (Any other numbers that may be assigned this report)
d.	

10. AVAILABILITY/LIMITATION NOTICES

Qualified requesters may obtain copies of this report from DDC.

This document has been approved for public release and sale; its distribution is unlimited

#1 Mgmnikan 12/22/69

11. SUPPLEMENTARY NOTES	12. SPONSORING MILITARY ACTIVITY
	U.S. Naval Postgraduate School Monterey, California

13. ABSTRACT

A system was designed to investigate experimentally the mechanism of nucleate pool boiling heat transfer using commercial grade liquid nitrogen as a working fluid. A circular horizontal flat plate five square centimeters in area was utilized as a boiler surface.

The effect of various surface parameters on the characteristic heat flux versus (T_W-T_S) curve at atmospheric conditions was determined. Surfaces used included a highly polished mirror surface, a mirror surface coated with oxide, a mirror surface coated with grease, a roughened surface, and a roughened surface coated with Teflon, all fabricated from commercial electrical tough pitch copper. The final surface used was a Nickel 200 highly polished mirror surface.

The data from the copper surface with a mirror finish was in agreement with the data of previous investigations. The effects of roughness, contaminants, hysteresis, and boiler surface material were discussed. A comparison was made on incipient boiling heat fluxes. The results indicate that the surface conditions play a major role in nucleate pool boiling heat transfer to liquid nitrogen.

DD FORM 1 JAN 64 1473

Security Classification

14. KEY WORDS	LINK A		LINK B		LINK C	
	ROLE	WT	ROLE	WT	ROLE	WT
Nucleate Boiling Cryogenic Surface Effects Flat Plate Boiler						

INSTRUCTIONS

1. ORIGINATING ACTIVITY: Enter the name and address of the contractor, subcontractor, grantee, Department of Defense activity or other organization *(corporate author)* issuing the report.

2*a*. REPORT SECURITY CLASSIFICATION: Enter the overall security classification of the report. Indicate whether "Restricted Data" is included. Marking is to be in accordance with appropriate security regulations.

2*b*. GROUP: Automatic downgrading is specified in DoD Directive 5200.10 and Armed Forces Industrial Manual. Enter the group number. Also, when applicable, show that optional markings have been used for Group 3 and Group 4 as authorized.

3. REPORT TITLE: Enter the complete report title in all capital letters. Titles in all cases should be unclassified. If a meaningful title cannot be selected without classification, show title classification in all capitals in parenthesis immediately following the title.

4. DESCRIPTIVE NOTES: If appropriate, enter the type of report, e.g., interim, progress, summary, annual, or final. Give the inclusive dates when a specific reporting period is covered.

5. AUTHOR(S): Enter the name(s) of author(s) as shown on or in the report. Enter last name, first name, middle initial. If military, show rank and branch of service. The name of the principal author is an absolute minimum requirement.

6. REPORT DATE: Enter the date of the report as day, month, year; or month, year. If more than one date appears on the report, use date of publication.

7*a*. TOTAL NUMBER OF PAGES: The total page count should follow normal pagination procedures, i.e., enter the number of pages containing information.

7*b*. NUMBER OF REFERENCES: Enter the total number of references cited in the report.

8*a*. CONTRACT OR GRANT NUMBER: If appropriate, enter the applicable number of the contract or grant under which the report was written.

8*b*, 8*c*, & 8*d*. PROJECT NUMBER: Enter the appropriate military department identification, such as project number, subproject number, system numbers, task number, etc.

9*a*. ORIGINATOR'S REPORT NUMBER(S): Enter the official report number by which the document will be identified and controlled by the originating activity. This number must be unique to this report.

9*b*. OTHER REPORT NUMBER(S): If the report has been assigned any other report numbers *(either by the originator or by the sponsor)*, also enter this number(s).

10. AVAILABILITY/LIMITATION NOTICES: Enter any limitations on further dissemination of the report, other than those imposed by security classification, using standard statements such as:

(1) "Qualified requesters may obtain copies of this report from DDC."

(2) "Foreign announcement and dissemination of this report by DDC is not authorized."

(3) "U. S. Government agencies may obtain copies of this report directly from DDC. Other qualified DDC users shall request through

_____."

(4) "U. S. military agencies may obtain copies of this report directly from DDC. Other qualified users shall request through

_____."

(5) "All distribution of this report is controlled. Qualified DDC users shall request through

_____."

If the report has been furnished to the Office of Technical Services, Department of Commerce, for sale to the public, indicate this fact and enter the price, if known.

11. SUPPLEMENTARY NOTES: Use for additional explanatory notes.

12. SPONSORING MILITARY ACTIVITY: Enter the name of the departmental project office or laboratory sponsoring *(paying for)* the research and development. Include address.

13. ABSTRACT: Enter an abstract giving a brief and factual summary of the document indicative of the report, even though it may also appear elsewhere in the body of the technical report. If additional space is required, a continuation sheet shall be attached.

It is highly desirable that the abstract of classified reports be unclassified. Each paragraph of the abstract shall end with an indication of the military security classification of the information in the paragraph, represented as *(TS)*, *(S)*, *(C)*, or *(U)*.

There is no limitation on the length of the abstract. However, the suggested length is from 150 to 225 words.

14. KEY WORDS: Key words are technically meaningful terms or short phrases that characterize a report and may be used as index entries for cataloging the report. Key words must be selected so that no security classification is required. Identifiers, such as equipment model designation, trade name, military project code name, geographic location, may be used as key words but will be followed by an indication of technical context. The assignment of links, roles, and weights is optional.

DD FORM 1 JAN 64 1473 (BACK)